Lab on a Chip

CRITICAL REVIEW

View Article Online
View Journal | View Issue

Open Access Article. Published on 09 September 2016. Downloaded on 1/4/2026 2:20:32 PM.
This article is licensed under a Creative Commons Attribution 3.0 Unported Licence.

Cite this: *Lab Chip*, 2016, **16**, 3664

Received 5th August 2016,
Accepted 23rd August 2016

DOI: 10.1039/c6lc01002d

www.rsc.org/loc

CMOS biosensors for *in vitro* diagnosis – transducing mechanisms and applications

Ka-Meng Lei,[ab] Pui-In Mak,*[ab] Man-Kay Law[a] and Rui P. Martins[abc]

Complementary metal oxide semiconductor (CMOS) technology enables low-cost and large-scale integration of transistors and physical sensing materials on tiny chips (*e.g.*, <1 cm^2), seamlessly combining the two key functions of biosensors: transducing and signal processing. Recent CMOS biosensors unified different transducing mechanisms (impedance, fluorescence, and nuclear spin) and readout electronics have demonstrated competitive sensitivity for *in vitro* diagnosis, such as detection of DNA (down to 10 aM), protein (down to 10 fM), or bacteria/cells (single cell). Herein, we detail the recent advances in CMOS biosensors, centering on their key principles, requisites, and applications. Together, these may contribute to the advancement of our healthcare system, which should be decentralized by broadly utilizing point-of-care diagnostic tools.

I. Introduction

An essential part of evaluating the success of global health is the access to appropriate diagnostic tools.[1] A commendable diagnostic tool should be able to rapidly identify disease occurring in individuals. Especially for infectious diseases, the turnaround time strongly affects their level of transmission to the community. *In vitro* diagnostic (IVD) tools aim to offer a comfortable experience for patients, by taking only a small specimen from the human body, *e.g.* blood, urine, sputum, and tissue. Consequently, technologies enabling effective *in vitro* diagnosis have become highly attractive in both developed and developing countries.[2] Tremendous efforts have been geared towards clinical-level IVD tools. Despite achieving high accuracy, the result turnaround time can be too long for contagious diseases like Ebola and SARS, and the need for skillful operators to perform the assays can dramatically raise the cost.

Recently, decentralized diagnostic solutions, namely point-of-care (PoC) devices, have gained notable interest, which is attributed to their rapidity, small footprint and tiny sample usage. A wide variety of diagnostic platforms have been invented, such as lateral flow assays[3–6] and the path-breaking lab-on-a-disc[7–10] for PoC applications. Beyond these, PoC devices on Complementary metal oxide semiconductor (CMOS) chips are particularly promising, as they can enjoy the maturity of microelectronics in manufacturing, and its outstanding performances in both physical sensing and signal processing. While the mainstream lateral flow assay is limited to providing merely qualitative or semi-quantitative results,[11] CMOS biosensors can attain quantitative results and are beneficial to rapid and low-cost assays. Especially for low-cost IVD applications, CMOS chips on a centimeter scale can significantly miniaturize diagnostic tools.

Decentralized healthcare systems are highly attractive for developing countries, which typically suffer from lack of access to high-quality centralized diagnostic tools. Delays in diagnosis and treatment aggravate the healthcare condition of these countries, thus affecting the global health system. According to the World Development Report in 2004, lack of access results in failure of health services.[12] Without proper equipment for diagnosis, diseases in resource-limited countries can only be diagnosed from their clinical symptoms. Yet, this may cause difficulties in diagnosing patients when their symptoms are still unobvious. Especially for infectious diseases, delays in treatment can worsen the situation of individuals, and consequently communities. According to a report by the World Health Organization (WHO), the leading infectious diseases (lower respiratory infections, HIV/AIDS, diarrhoeal diseases, malaria, and tuberculosis) account for roughly one-third of all deaths in low-income countries.[13] Also, the strong growth in population in these areas gives rise to the demand for affordable IVD tools. By the end of 2050, the less-developed countries are expected to have a population of around 8.4 billion, as depicted in Fig. 1(a), where Africa and Asia contribute roughly 2.48 and 5.27 billion, respectively.[14] Thus, there is a rapidly growing market for low-cost PoC devices for developing countries.

[a] *State-Key Laboratory of Analog and Mixed-Signal VLSI, University of Macau, China. E-mail: pimak@umac.mo*
[b] *Faculty of Science and Technology, Dept. of ECE, University of Macau, China*
[c] *On leave from Instituto Superior Técnico, Universidade de Lisboa, Portugal*

This journal is © The Royal Society of Chemistry 2016

Open Access Article. Published on 09 September 2016. Downloaded on 1/4/2026 2:20:32 PM.
This article is licensed under a Creative Commons Attribution 3.0 Unported Licence.

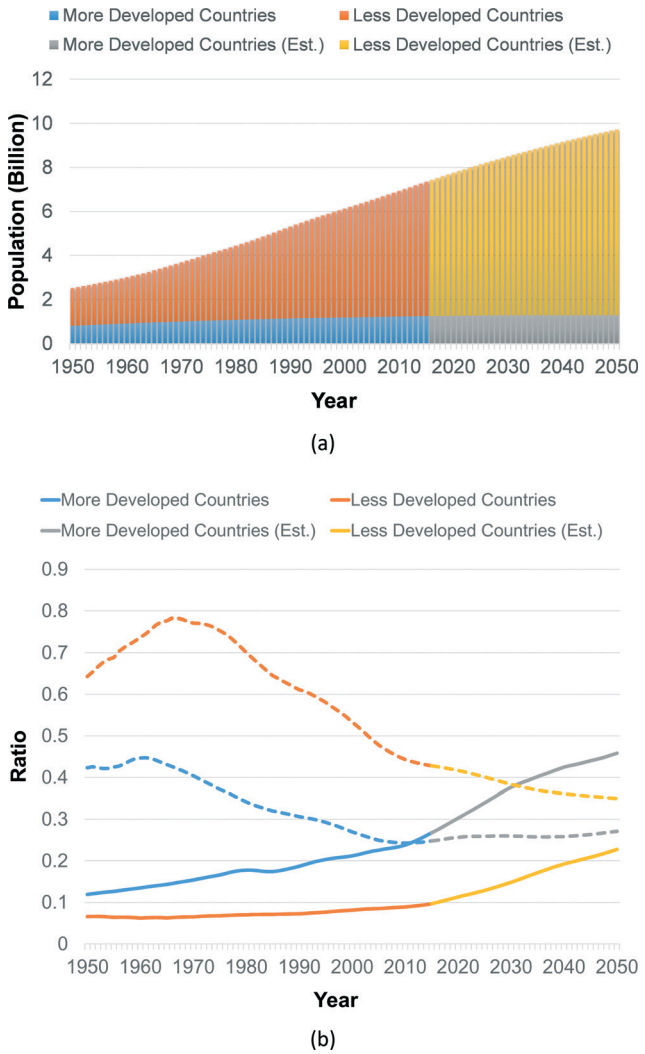

Fig. 1 (a) World population from 1950 to 2050, with a medium variant estimation from 2015. (b) The old-age dependency ratio (solid line), which is defined as the ratio of the population of 65+ year olds to the population of 15 to 64 year olds with a medium variant estimation from 2015. The child dependency ratio (dotted line), which is defined as the ratio of the population of 0 to 14 year olds to the population of 15 to 64 year olds, is also shown on the graph as reference. Data collected from the United Nations *World Population Prospects: The 2015 Revision.* More developed countries: Europe, Northern America, Australia/New Zealand, and Japan. Less developed countries: Africa, Asia (except Japan), Latin America, and the Caribbean, plus Melanesia, Micronesia and Polynesia.

The aging problem of developed countries also creates an enormous challenge. A healthcare solution that can deal with the continuous increase in longevity is in demand. As revealed in Fig. 1(b), the old age dependency ratio, which gives an insight into the elderly population (65+ years) compared to those of working age (15 to 64 years), will be rising in the coming decades. Such an old-age dependency ratio in more developed countries will reach 0.4 in 2034, and eventually 0.46 by the end of 2050 (*i.e.*, an increase of 72% from 2015). Thus, the burden on the clinical resources in those areas will become tighter, especially for the patients in close proximity to death.[15] Thus, an efficacious healthcare system will benefit this situation, and drive the growth of the market for IVD tools. To this end, the market for IVD tools should not be merely aimed at less developed countries, but also towards efficient and convenient diagnosis in developed countries. In fact, according to a report from Forbes/Investing, the IVD market, valued at ~$50 billion in 2012, will expand to ~$70 billion by 2017.[16] This paper studies and compares state-of-the-art CMOS biosensors tailored for *in vitro* diagnosis, including primarily the assay or monitoring of DNA, proteins, and cells. For the readout electronics of CMOS biosensors (*e.g.*, amplifiers, filters, and oscillators), we refer readers to literature that emphasizes circuit-level challenges and realization.[17,18] There are also review articles focusing on the system-level aspects of general PoC devices (not limited to CMOS), which discuss the design criteria and system requirements.[2,19–27] Herein, we focus in detail on the *transducing mechanisms* of CMOS chips that could open up many possibilities for *in vitro* diagnosis.

After the introduction, different transducing mechanisms of CMOS PoC devices for biological sensing and targeting, namely electrical, magnetic, optical, mechanical, and nuclear spin, will be revealed. Then, different CMOS IVD tools for various targets of interest, such as DNA, protein and cells/bacteria will be discussed. Their pros and cons will be outlined and compared, offering the readers a systematic outlook on their distinct characteristics and limitations.

II. Transducing mechanisms of CMOS IVD tools

Rapid downscaling of CMOS technology has allowed the possibility of integrating billions of transistors onto a single chip, allowing ultra-fast signal processing at low power and cost. While their transformative effects on computers and mobile devices have been witnessed, the development of CMOS PoC devices for *in vitro* diagnosis only started recently. Along with circuit innovation, high-sensitivity analog interfaces are ready for CMOS biosensors. Thus, single-chip CMOS biosensors allow full integration of the transducers and circuits necessary for signal processing. This property aligns with the expectations for PoC devices, such as low sample consumption, small footprint, ease of use, and rapid and quantitative results. Attributed to the design flexibility of CMOS chips, multifarious CMOS biosensors have been reported, as listed in Table 1. Also, the capability to include post-processing steps (*e.g.*, chemical deposition and micromachining) after chip manufacturing can help in broadening the versatility of CMOS biosensors.[28–33]

According to their transducing mechanisms, CMOS PoC devices can be classified as: 1. electrical-based – directly sensing the electrical properties of samples, such as impedance or electric charges (currents); 2. optical-based – transducing the optical properties from the samples, such as fluorescence labels or chemiluminescence, into an electrical signal; 3. magnetic-based – transducing the magnetic properties of the

Open Access Article. Published on 09 September 2016. Downloaded on 1/4/2026 2:20:32 PM.
This article is licensed under a Creative Commons Attribution 3.0 Unported Licence.

Table 1 Recent CMOS biosensors for different applications

Targets	Applications	Sensing parameters	Transducers	Labeling	Immobilization	Lowest amount reported	Year
DNA	DNA detection	Capacitance	Au electrodes	Label-free	Yes	N/A	2006 (ref. 34)
	DNA detection	Charge	ISFET	Label-free	Yes	0.1 mM	2006 (ref. 35)
	DNA detection	Magnetism	Spin-valve sensors	Magnetic particle (target)	Yes	10 nM	2007 (ref. 36)
	DNA polymerization	Charge	Polymer + metal	Label-free	Yes	N/A	2008 (ref. 37)
	DNA detection	Fluorescence	Photodetector	Cy-3 label (target)	Yes	0.125 nmol	2009 (ref. 38)
	DNA detection	Fluorescence	Photodetector	Biotin and Qdot-655 (target)	Yes	4 nM	2009 (ref. 39)
	DNA detection	Magnetism	LC-oscillator	Digoxigenin & magnetic particle (target)	Yes	1 nM	2009 (ref. 40)
	DNA detection	Cyclic voltammetry	Au electrodes	Ferrocene redox label (target)	Yes	4 nM	2009 (ref. 41)
	DNA detection	Impedance	Au electrodes	Label-free	Yes	N/A	2010 (ref. 42)
	DNA detection	Impedance	Au electrodes	Label-free	Yes	5 μM	2012 (ref. 43)
	DNA detection	Capacitance	Au electrodes	Label-free	Yes	100 pM	2012 (ref. 44)
	DNA detection	Charge	Au electrodes	Label-free	Yes	100 pM	2012 (ref. 45)
	DNA detection	Mass	Cantilever	Label-free	Yes	1 pM	2013 (ref. 46)
	DNA amplification & detection	Charge	ISFET	Label-free	No	10 copies	2013 (ref. 47)
	DNA detection	Charge	Silicon nanowire	Label-free	Yes	3.2 pM	2013 (ref. 48)
	DNA detection	Magnetism	LC-oscillator	Magnetic particle (probe)	Yes	100 pM	2014 (ref. 49)
	DNA detection	Cyclic voltammetry	Au electrodes	Label-free	Yes	10 aM	2014 (ref. 50)
	DNA amplification & detection	Fluorescence	SPAD	EvaGreen® dye	No	1 copy	2014 (ref. 51)
	DNA detection	Nuclear spin	Spiral coil	Magnetic particle (probe)	No	50 pM	2016 (ref. 52)
Protein	C-reactive protein	Mass	Cantilever	Label-free	Yes	1 μg mL^{-1}	2009 (ref. 53)
	Avidin	Nuclear spin	Spiral coil (off-chip)	Magnetic particle (probe)	No	5 nM	2009 (ref. 54)
	hMAM cancer marker	Mass	SAW transducer	Label-free	Yes	1.5 μg mL^{-1}	2010 (ref. 55)
	Protein G	Impedance	Au electrodes	Label-free	Yes	N/A	2010 (ref. 42)
	hCG cancer marker	Nuclear spin	Spiral coil	Magnetic particle (probe)	No	5 nM	2011 (ref. 56)
	Human serum albumin	Magnetism	Hall sensor	Magnetic particle (probe)	Yes	1 ng mL^{-1}	2013 (ref. 57)
	SLPI cancer marker	Magnetism	GMR spin-valve sensor (off chip)	Magnetic particle (probe)	Yes	10 fM	2013 (ref. 58)
	Cardiac troponin I protein	Charge	Silicon nanowire	Label-free	Yes	10 fM	2013 (ref. 48)
	Cytokines (IL8, IFN, TNFα)	Chemiluminescence	Photodetector	Horseradish peroxidase	Yes	3 pg mL^{-1}	2014 (ref. 59)
	C-reactive protein	Capacitance	Au electrodes	Label-free	Yes	0.5 mg L^{-1}	2015 (ref. 60)
	Streptavidin	Fluorescence	Photodetector	Qdot 800 fluorophore	Yes	48 zmol	2015 (ref. 61)
	TNF-alpha & NT-probnp	Magnetism	Hall sensor	Magnetic particle (probe)	Yes	0.8 pg mL^{-1}	2015 (ref. 62)

 This journal is © The Royal Society of Chemistry 2016

Open Access Article. Published on 09 September 2016. Downloaded on 1/4/2026 2:20:32 PM.
This article is licensed under a Creative Commons Attribution 3.0 Unported Licence.

Table 1 *(continued)*

Targets	Applications	Sensing parameters	Transducers	Labeling	Immobilization	Lowest amount reported	Year
	Multi-analyte	Chemiluminescence	Photodetector	Horseradish peroxidase	Yes	45 ng mL^{-1} ferritin	2015 (ref. 63)
	Human IgG	Nuclear spin	Spiral coil	Magnetic particle (probe)	No	5 nM	2016 (ref. 52)
	Mouse IgG	Magnetism	Microcoil (off-chip)	Magnetic particle (probe)	Yes	100 pg mL^{-1}	2016 (ref. 64)
Cells/bacteria	Bovine aortic smooth muscle cell monitoring	Capacitance	Metal electrodes	Label-free	No	20 × 20 μm^2	2007 (ref. 65)
	MDA-MB-231 breast cancer cell monitoring	Capacitance	Metal electrodes	Label-free	No	20 × 20 μm^2	2008 (ref. 66)
	Bladder cancer cell detection	Nuclear spin	Spiral coil	Magnetic particle (probe)	No	17.5 cells per μL	2011 (ref. 56)
	MCF-7 breast cancer cell detection	Fluorescence	SPAD	5D10 monoclonal antibody	No	Single cell	2012 (ref. 67)
	MCF-7 breast cancer cell detection	Impedance	Au electrodes	Label-free	No	Single cell	2012 (ref. 68)
	RBC flow cytometer	Impedance	Metal electrodes	Label-free	No	Single cell	2012 (ref. 69)
	Cardiac progenitor cell monitoring	Magnetism	LC-oscillator	Magnetic particle (target)	No	N/A	2012 (ref. 70)
	HeLa cell counting	Optics	CMOS image sensor	Label-free	No	25 cells per mL	2014 (ref. 71)
	Mouse embryonic fibroblast cell	Magnetism	Excitation & pickup coils	Magnetic particle (target)	No	Single cell	2014 (ref. 72)
	Complete blood count	Optics	CMOS image sensor	Label-free	No	N/A	2014 (ref. 73)
	HeLa cell counting	Cyclic voltammetry	Au electrodes	Label-free	No	N/A	2015 (ref. 74)
	MCF7, BEAS, & K562 cancer cell monitoring	Capacitance	Au electrodes	Label-free	No	N/A	2015 (ref. 75)
	Multiple cell monitoring	Multi-modal	Au electrodes & photodetector	Label-free	No	N/A	2015 (ref. 76)
	HepG2 cancer cell monitoring	Optics	CMOS image sensor	Label-free	No	5000 cells per mL	2015 (ref. 77)

samples arising from labeled magnetic particles (nano-particles) into an electrical signal; 4. mechanical-based – transducing the mechanical properties, namely the mass of the targets, to an electrical signal; 5. nuclear magnetic resonance (NMR)-based – transducing the nuclear spin from the sample, which is affected by the magnetic susceptibility, to an electrical signal. Details of each transducing mechanism and its corresponding example from Table 1 will be presented next.

Electrical-based

The capability of the CMOS chip to seamlessly handle electrical signals, such as current, impedance and capacitance, is ascribed to direct electronic detection biosensors, which are the most popular type of CMOS biosensors for *in vitro* diagnosis [Fig. 2(a)]. The electrical properties serve as a reliable measure to quantify the concentration of analyte inside the samples. The electrode acting as substrate for probe immobilization is usually formed by the top metal layer, which offers great feasibility for the downscaling of CMOS technologies, and is expandable to form an array for multi-targeting.

A popular approach is electrochemical impedance spectroscopy (EIS), where the impedance between the electrodes is monitored over a range of frequencies. This provides details of the impedance changes of the solution and the electrode-solution interface. EIS has been involved in detecting affinity-based biosensing, which explores the binding events between the probe (*i.e.*, complementary oligonucleotides, antibody/antigen) and the target within the samples. The probe can be immobilized on the electrodes with special chemical post-processing.[78] Upon hybridization between the probe and target, the double-layer capacitance of the electrode-electrolyte interface decreases due to the increased thickness, together with the decreased dielectric constant, whereas the charge-transfer resistance increases, since the attached target partially blocks the flow of the ions.[79] Thus, the system is capable of quantifying the analyte of interest by detecting the impedance between the electrodes. For instance, Manickam *et al.* showed a versatile EIS biosensor array on a CMOS chip.[42] This fully integrated and label-free detecting platform is capable of quantifying different DNA and protein targets inside the samples with corresponding immobilized probes

Open Access Article. Published on 09 September 2016. Downloaded on 1/4/2026 2:20:32 PM.
This article is licensed under a Creative Commons Attribution 3.0 Unported Licence.

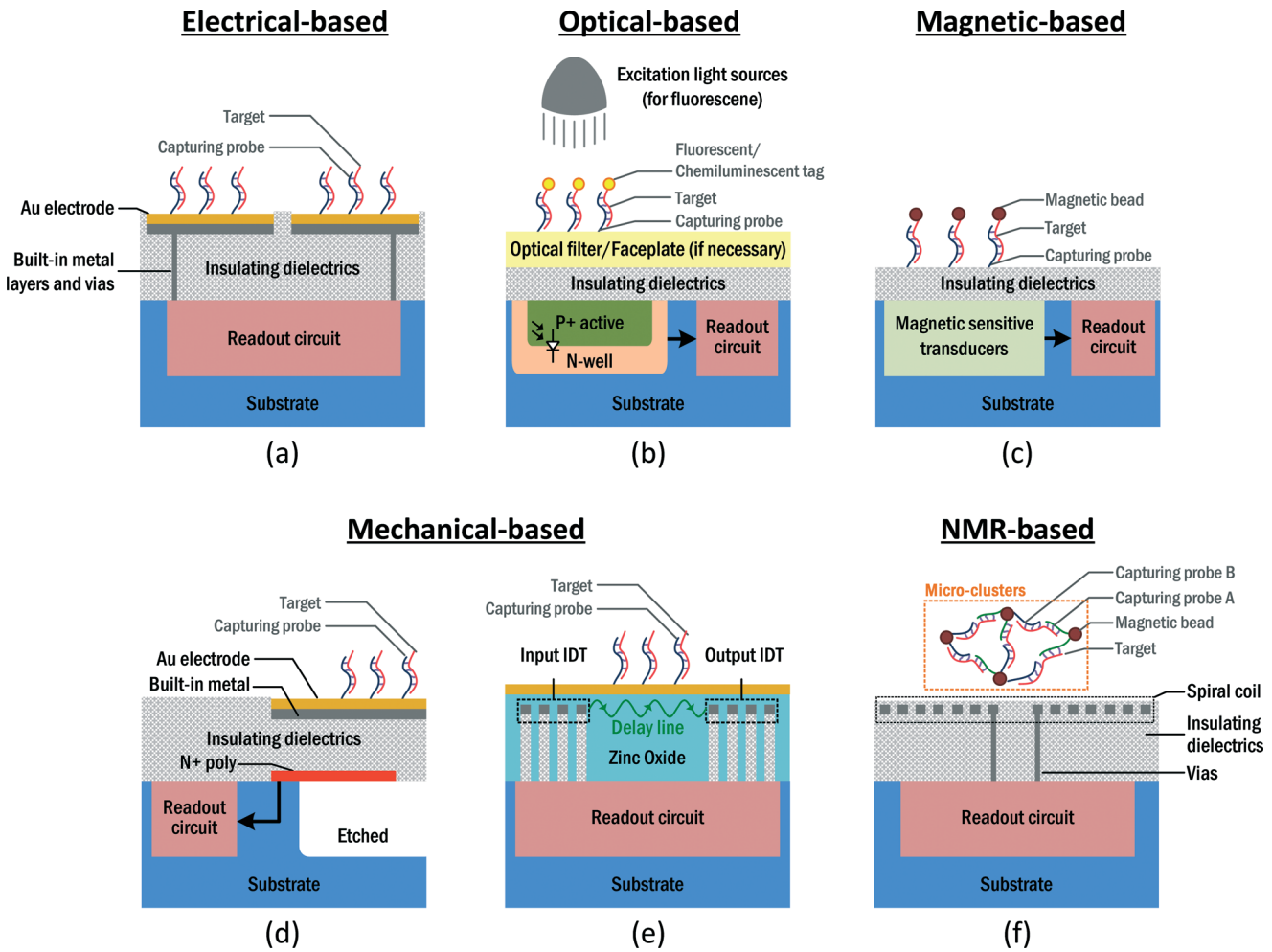

Fig. 2 Architecture and operation of different CMOS biomolecule transducing mechanisms. (a) Electrical-based detection (excluding the FET-type biosensors). An extra layer of noble and biocompatible metal, such as gold, is deposited on the original built-in metal layer. The capturing probe is then immobilized on the gold electrode to capture the target. Upon hybridization, the electrical properties, such as impedance or charge, are sensed directly by the readout circuit. (b) Optical-based detection. The capturing probe is immobilized on a solid substrate, such as glass or the built-in passivation layer atop the CMOS chip. Then, a fluorescence-labeled or chemiluminescence-labeled target will bind with the probe and other unbound biomolecules will be washed away. The CMOS photodetector, which is formed by the embedded PN-junction, transduces the optical signal to current for subsequent signal processing. (c) Magnetic-based detection. The capturing probe is immobilized on a solid substrate, such as glass or the built-in passivation layer atop the CMOS chip. Then, the sample labeled with magnetic particles will mix with the capturing probe. The matched target will be captured and unbound objects will then be rinsed off. A magnetic transducer, such as an LC-oscillator or Hall sensor will transduce the magnetism of the sample to electrical signals, which will be subsequently processed by the readout circuit. (d) Mechanical-based detection with cantilever. A cantilever can be exploited to transduce the mass attached to it to electrical signals, such as resistance. A gold layer is deposited on the cantilever for growing the capturing probe on it. In order to allow the cantilever to bend upon attaching the biomolecule, the neighbouring insulating dielectrics and the base of the cantilever are etched away. A piezoresistor can be adopted to transduce the bending force on the cantilever to a resistance change, and the readout circuit will detect this variation. (e) Mechanical-based detection with SAW transducer. A complete SAW transducer consists of three modules, the input metal interdigital transducer (IDT), the piezoelectric delay line, which the acoustic wave travels through, and the output metal IDT. The input IDT generates the SAW. Then, the wave travels through the delay line to the output IDT, where the SAW is transduced back to the electrical signal. The bio-functionalized gold layer atop the delay line captures the entity under analysis. The increased mass here will affect the characteristics of the delay line, resulting in a change in resonant frequency, amplitude, or phase shift on the SAW, which can then be detected on the output IDT. (f) NMR-based detection. NMR focuses on the measurement of the NMR signals from the samples. First, the magnetic particle functionalized with the capture probes reacts with the sample under analysis. Then, the mixture will be placed atop the spiral sensing coil to perform the NMR experiment. The existence of a target inside the sample incurs particle aggregation, thus a larger micro-cluster will be formed, changing the spin–spin relaxation time of the NMR signal from the sample.

on the electrodes. Alternatively, the capacitance between the electrodes can also be used to detect the target upon the hybridization of DNA.[80] Lee *et al.* reported a CMOS label-free capacitive biosensor for detecting DNA from the H5N1 virus.[44] Instead of observing the complex impedance of the electrodes, this capacitive biosensor only focuses on the measurement of the capacitance of the electrodes, thus the circuit design can be simplified. The capacitive sensing mechanism is also an adequate candidate for cell monitoring. Prakash *et al.* presented a CMOS platform for cancer cell

 This journal is © The Royal Society of Chemistry 2016

Open Access Article. Published on 09 September 2016. Downloaded on 1/4/2026 2:20:32 PM.
This article is licensed under a Creative Commons Attribution 3.0 Unported Licence.

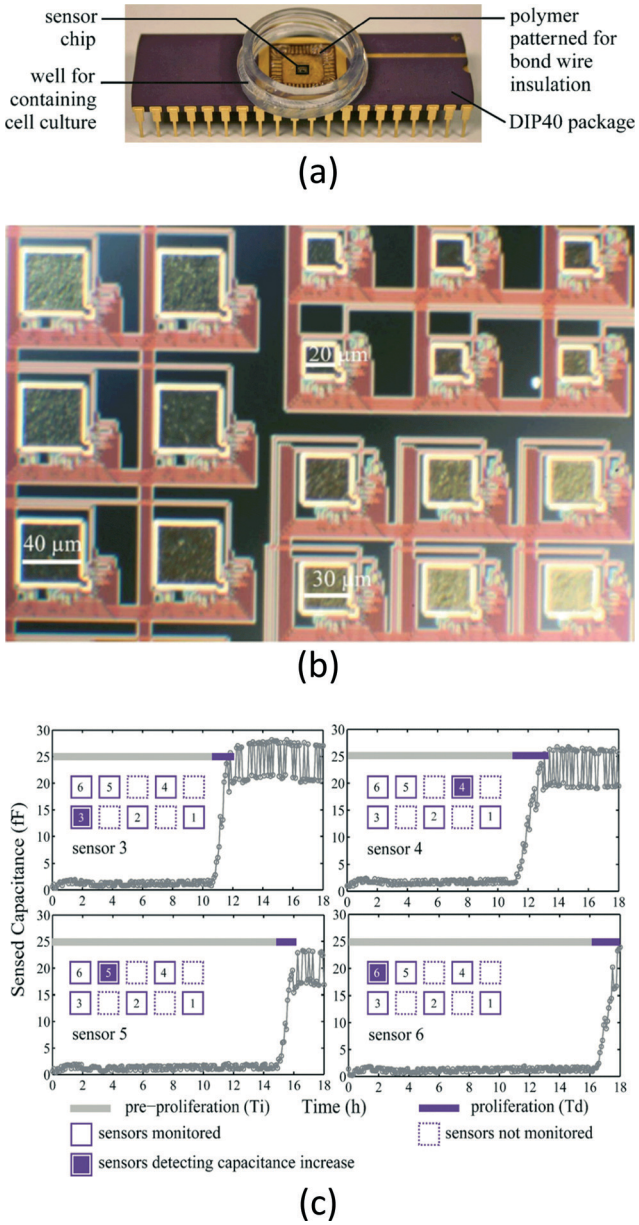

Fig. 3 Cell culturing and monitoring with CMOS capacitive sensing chip. (a) A photograph showing the overall chip with dual in-line package. A well encloses the cell culturing site and the CMOS chip is in the center of the well. The bond wires of the chip are protected by the polymer. (b) Photomicrograph of the electrode. Since the system measures only the capacitance of the single electrode, the built-in passivation layer, such as silicon nitride and silicon dioxide, can be preserved without further post-processing. This simplifies the hardware preparation steps for biosensing. (c) The experimental results for cancer cell MDA-MB-231 culturing. The capacitance at a specific site increases due to the proliferation of the cancer cells, ascribed to the increased number of cells, allowing real-time monitoring of the growth of the cancer cells. Reproduced with permission from ref. 66. Copyright 2008 Elsevier.

MDA-MB-231 proliferation monitoring [Fig. 3(a)].[66] Since the capacitance can be sensed without removing the passivation layer, post-processing on the CMOS chip can be obviated [Fig. 3(b)]. The underlying principle is the insulating nature of the cell, together with the counterionic polarization in the surrounding aqueous medium on exposure to low-frequency electric fields, which accounts for the capacitive behavior of the cell [Fig. 3(c)].

Alternatively, voltammetric, amperometric and potentiometric techniques monitor the electrochemical reactions (*i.e.*, charge transfer) within the samples directly. These electrochemical reactions are related to the concentration of the analytes. With a specific readout circuit, such as a potentiostat, these electrochemical reactions can be measured and the concentration of the biomolecule can be quantified. Levine *et al.* described a CMOS multiplexed electrochemical microsystem with a 4 × 4 electrode array for DNA detection.[41] By sweeping the voltage between the electrodes, the current produced by a redox label on the target DNA sequence can be recorded by the on-chip electronics.

With the advance of post-processing in standard CMOS chips, special field-effect transistor (FET) biosensors, which sense the charges of ions/electrons from the target, such as ion sensitive FETs (ISFETs)[35] and silicon nanowire (NW),[33,48] also show promise for biomolecule detection. Compared to the standard electrical-based biosensors shown in Fig. 2(a), these have a different architecture and usually require further post-processing. Their operations are similar to MOSFET: the target concentration alters the charges on the surface of the FET, thus the physical properties of the channel are altered. For instance, Huang *et al.* reported a CMOS wireless biomolecular sensing system based on polysilicon NW.[48] The resistance of the n-type doped polysilicon NW decreases upon the hybridization of complementary DNA on the NW, since the electrons in the NW are repelled from the surface. Thus, by detecting the resistance of the NW, the quantity of DNA inside the samples can be identified.

Optical-based

As the dominant detection modality for existing diagnostic tools is within the visible range of fluorescence spectroscopy, optical sensing still plays an important role in CMOS biosensing platforms, since conventional immunoassay protocols, such as ELISA, can migrate to the CMOS chip. The principle of fluorescent biomolecule assay is the detection of a fluorescence signal from a labeled fluorescent tag after washing the unconjugated tag. Upon excitation from an external light source, these fluorescent labels emit a signal at a longer wavelength due to Stokes shifting. Then, the designated transducer, such as a photodetector, which is implemented by an embedded PN-junction available in the standard CMOS process, can collect these signals and transduce them to the electrical domain (*i.e.*, voltage or current) for signal amplification and conditioning [Fig. 2(b)].

In order to integrate the fluorescence module into a CMOS chip, several considerations have to be taken into account. Firstly, since the signals are in the optical domain, the metal layers above the photodetector should be avoided to prevent blocking the signal. Secondly, as the intensity of the excitation signal is usually much stronger than the fluorescent

Open Access Article. Published on 09 September 2016. Downloaded on 1/4/2026 2:20:32 PM.
This article is licensed under a Creative Commons Attribution 3.0 Unported Licence.

signal, its presence at the photodetector will saturate it, thus causing system malfunctioning. Jang *et al.* proposed a CMOS fluorescence-based biosensor microarray for DNA detection.[38] To filter the excitation signal and prevent it from reaching the photodetector, a separate 20 layer thin-film long-pass optical filter has to be put atop the CMOS chip. This filter rejects the excitation signal at 532 nm by 98 dB, while preserving a low passband attenuation of 1 dB. Furthermore, to direct the fluorescence signals with the photodetector, a fiber-optical faceplate was fabricated to guide the signals along the vertical direction. These CMOS-incompatible modules restrict the integration and raise the system cost. To this end, Huang *et al.* proposed an integrated time-resolved fluorescence detection CMOS array sensor suitable for DNA detection.[39] Instead of removing the excitation signal by an optical filter, the proposed system adopts a time-gated arrangement to monitor the fluorescent decay of the labels after excitation. This scheme leads to a high signal-to-background ratio without any external filters. Lately, a fully integrated CMOS fluorescence biosensor with an on-chip nanophotonic filter was proposed.[61] The design included an integrated optical filter obtained with back-end-of-line copper layers. This filter can suppress the excitation light without any external filtering/collimation, facilitating the integration of the entailed CMOS electronics and optical filters for fluorescent assays.

Similar to fluorescent detection, the chemiluminescent signal can also be detected from the signaling tag with a photodetector. The chemiluminescent tag, which emits a light signal based on the chemical reaction, averts the external light source to excite them. This prevents the saturation of the photodiode. Furthermore, the avoidance of an optical filter shortens the distance from the signaling tag to the surface of the photodetector, which fulfills the criteria for supercritical angle luminescence (SAL) and enables efficient signal detection.[81] Sandeau *et al.* proposed a large-area CMOS bio-pixel array for multiplex biosensing.[59] The high refraction index of the silicon substrate enables the SAL phenomenon and thus the direction of light emission from the chemiluminescent tag is confined to the surface, and the sensitivity is boosted by 100 fold compared to the standard microplate reader.

For larger biological objects, such as cells and bacteria, direct optical detection without a labeling tag is also feasible by using a high-speed CMOS image sensor. With the advance of CMOS imaging technologies, real-time cell monitoring and counting can also be achieved on a CMOS chip directly. The appearance of the objects blocks the photon from arriving at the CMOS image sensor, thus the system can count and monitor the activity of the cells/bacteria. Different cell monitoring systems based on CMOSs have been described in the literature. Saeki *et al.* proposed a lens-free cell counting device for HeLa cells with a microcavity array[71] [Fig. 4(a) and (b)]. The cells are trapped on the microcavity array by applying a negative pressure underneath. Hence, the cells trapped inside the microcavity block the light from the light emitting diode and create a shadow on the CMOS image sensor, thus the CMOS image sensor can enumerate the cells on the array [Fig. 4(c) and (d)].

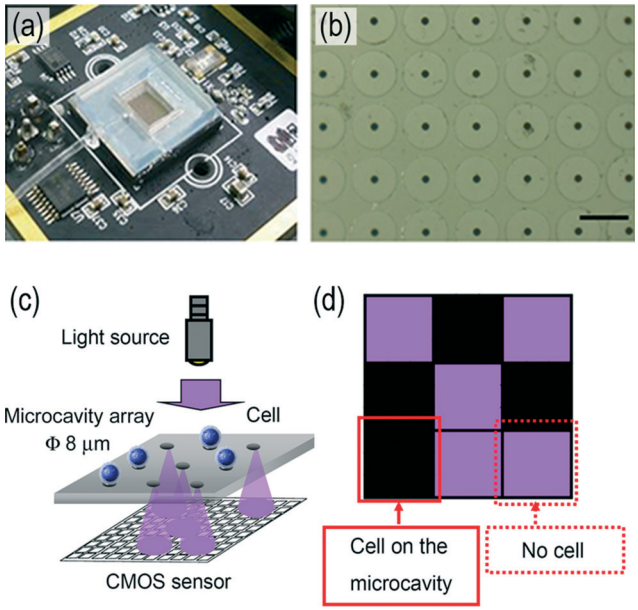

Fig. 4 Lens-free cell/micro-particle counting system with CMOS image sensor. (a) The overall platform of the digital cell counting device. (b) A micrograph of the microcavity array for cell trapping. The sample under analysis is put atop the micro-cavity array. Then, the suspended cells/micro-particles will be pulled toward and trapped in the cavities by the negative pressure. This negative pressure is produced by a peristaltic pump, which extracts the air inside the chamber. (c) Detection principle of the system. The light from the external UV light source will arrive at the CMOS image sensor through the unoccupied cavity, while the trapped cell on the cavity blocks the light from arriving at the CMOS image sensor. (d) The schematics of the expected CMOS image acquired from (c). Since the cell blocks the UV light from passing through the cavity, the pixels under the occupied cavity will report a darker region, while the pixels under the vacant cavity will report a brighter result. Thus, the number of cells on the microcavity array can be identified from the result from the CMOS image sensor. Reproduced with permission from ref. 71. Copyright 2014 Saeki *et al.*

Magnetic-based

Magnetism has recently become a tantalizing mechanism for biomolecule detection. Ascribed to the absence of magnetic signal in the sample and background, magnetism originating from the labeled magnetic micro- or nano-particles can be clearly detected from the samples. In addition, as the magnetic field can penetrate the insulating dielectric layers, direct contact between the samples and the transducers is avoided. This simplifies the hardware preparation of the CMOS chip before the assay. The basic operation is to grow an immobilization layer on a surface proximal to the transducer, similar to the electrical- and optical-based biosensors. Then, the magnetic-labeled sample can be placed on the transducer for hybridization. After a washing step to flush the unbound biomolecules and magnetic particles, the target of interest with magnetic particles will stay on the surface, allowing the transducer to detect the corresponding signal if the target exists inside the sample [Fig. 2(c)].

 This journal is © The Royal Society of Chemistry 2016

Open Access Article. Published on 09 September 2016. Downloaded on 1/4/2026 2:20:32 PM.
This article is licensed under a Creative Commons Attribution 3.0 Unported Licence.

There are diverse transducers to convert this magnetism to an electrical signal. For instance, a Hall sensor can be adopted to sense the magnetic field and transduce it to voltage/current signals. The Hall sensor, composed of n-type silicon, can offer moderate mobility (*i.e.*, sensitivity) yet be fully compatible with the CMOS process. The current carriers in the sensor experience a Lorentz force when there is a magnetic field orthogonal to the direction of current flow applied to them. This causes charge deflection and allows electronic detection. Gambini *et al.* proposed a CMOS Hall sensor array for immunoassays.[57] A Hall sensor was adopted to perform the relaxation measurement on the magnetic field and transduce this to a voltage signal. With the bound magnetic particles, the relaxation of the magnetic field from the particles relaxes to zero, according to the Néel relaxation mechanism. Thus, by detecting this relaxation time, the concentration of the magnetic particles (*i.e.*, the target concentration) can be detected. Alternatively, an inductor can also be employed to sense the magnetism of the samples. As the inductance is heavily affected by the proximal magnetic susceptibility, the target can be quantified by detecting its inductance. Pai *et al.* presented a CMOS magnetic biosensor array for DNA and protein detection using an embedded LC-oscillator (L and C represent the inductor and capacitor), where the inductor implementation uses the top metal layer of the CMOS chip [Fig. 5(a)–(c)].[49] The bound magnetic particles are detected from the oscillation frequency of the oscillator. They demonstrated the detection of DNA with a concentration of 100 pM by a novel magnetic freezing technique to reduce the sensor noise [Fig. 5(d)].

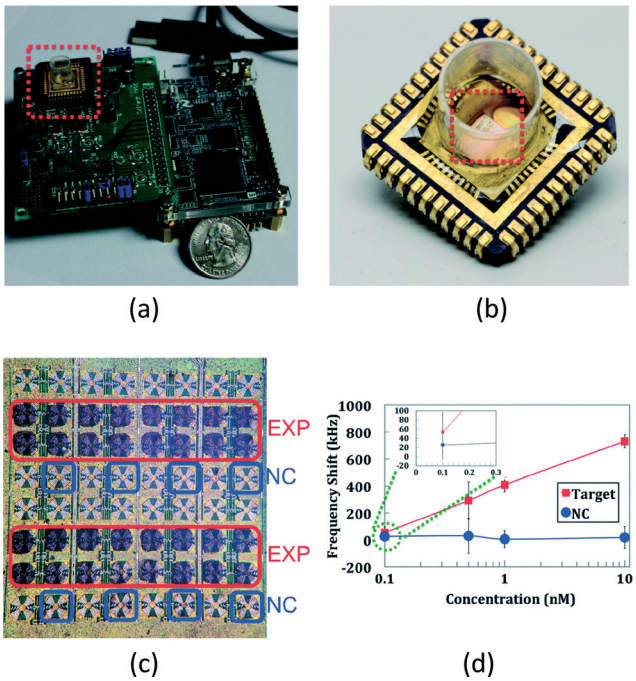

Fig. 5 magnetic-based handheld diagnostic device for antigen and nucleic acid detection. (a) The overall platform of the diagnostic device. The CMOS chip is easily plugged in on the print circuit board with a cartridge. (b) The disposable cartridge with the CMOS chip. The CMOS chip is attached to the cartridge with silver epoxy and connected with bond wire to the carrier leads. This arrangement enables a disposable, low-cost and multiplexed assay, and simplifies the sample handling module, such as microfluidic, to manage the sample to the sensing sites. (c) The CMOS chip. It has 48 on-chip sensing sites, together with 16 reference sensors. Each coil, together with its own capacitor, forms an LC-oscillator, which has an oscillating frequency inversely proportional to the square root of the inductance of the coil. The surface of the chip is biofunctionalized for probe immobilization. The sample with the magnetic particle is then applied on the surface of the chip, followed by a washing step to rinse the unbound molecules and magnetic particles. The bound magnetic particles increase the inductance of the coils, thus by detecting the oscillation frequency, the concentration of the target at a specific site can be selectively evaluated. (d) The experimental results for DNA detection. The frequency shift of the oscillation frequency is commensurate with the concentration of the target. With the novel magnetic freezing scheme, a limit-of-detection of 100 pM DNA can be achieved. Reproduced with permission from ref. 49. Copyright 2014 RSC Publishing.

Mechanical-based

Mass is a fundamental parameter for analyzing the concentration of a target by utilizing an immobilized probe on the transducer without a labeling process. The probes capture the targets in the samples and thus the mass on the transducer increases. Then, a specific transducer converts the mass variation to an electronic signal.

An example of this kind of mechanical transducer is the cantilever [Fig. 2(d)]. This senses the concentration of the analyte by the mass attached to the cantilever, and it is designed to work in a static or dynamic mode.[82] In the static mode, only one surface of the cantilever is bio-functionalized and thus bending occurs statically in one direction. While working in the dynamic mode, the entire cantilever operates in the capture of the targets, with its resonant frequency sensitive to the mass attached. By adopting a special design and post-processing, such as etching and additional layer depositing, the CMOS chip is capable of embodying a cantilever and transduces the mass attached to electrical signals. If the targets are presented in the samples, the probe will seize the targets, raising the mass of the cantilever as a mechanical effect. This event can be detected from the resistance, resonant frequency, or optical deflection of the cantilever, depending on the design and criteria of the platforms. Chen *et al.* demonstrated a silicon-based micro-cantilever to detect C-reactive protein from a sample.[53] The deflection ascribed to the additional mass on the cantilever is detected by the displacement of an optical beam, which is reflected by the surface of the cantilever and detected by another photodetector chip. Yet, the separate modules and the inclusion of the optical gadgets (*i.e.*, laser beam generator, lens and mirror) restrict the integration of the systems, and reduce their applicability outside the laboratory. Subsequently, an integrated cantilever system-on-chip for label-free DNA hepatitis B virus detection was proposed by the same group.[46] In this work, the deflection of the cantilever is detected by an embedded n+ polysilicon piezoresistor, whose resistance varies depending upon the

Open Access Article. Published on 09 September 2016. Downloaded on 1/4/2026 2:20:32 PM.
This article is licensed under a Creative Commons Attribution 3.0 Unported Licence.

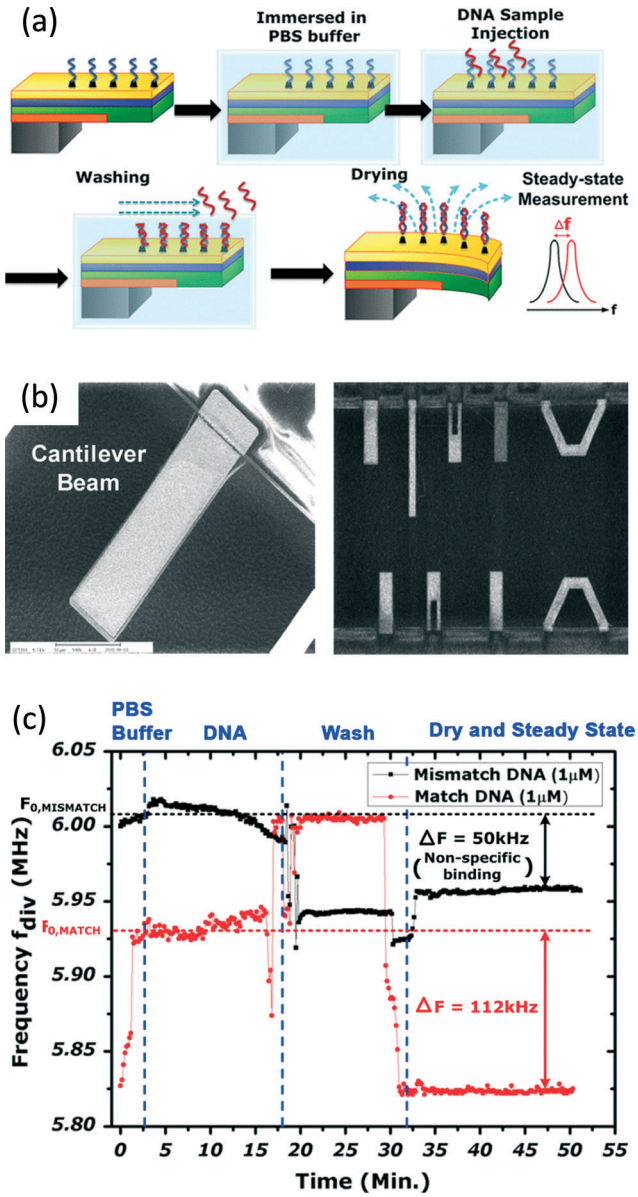

Fig. 6 A CMOS cantilever-based biosensor for DNA detection. (a) The operation procedures of the biosensor. After post-processing to implement the cantilever on the CMOS chip, the captured DNA is immobilized on the Au surface of the cantilever. Then, the cantilever is immersed in the PBS buffer and the sample of interest is injected around the cantilever to allow hybridization of DNA. After washing off the unbound biomolecules, the cantilever is left to dry. After all of the water molecules are evaporated, the matched target DNA will stay on the Au surface. Their masses incur bending of the cantilever and an embedded piezoresistor implemented by N+ polysilicon is entailed to sense this bending, and transduce it to variation of its own resistance, causing a frequency shift on the ring-type oscillator. (b) An SEM image showing the cantilevers. In order to allow the cantilever to bend freely in air, the surrounding materials, such as the insulating dielectrics and p-substrate underneath, have to be etched away, creating a suspended cantilever. (c) Experimental results for the biosensor. The resistance variation of the polysilicon piezoresistor, attributed to the bending of the cantilever, incurs a deviation of the oscillating frequency. After DNA sample injection, and washing and drying steps, the final steady-state frequency can be measured to selectively quantify the concentration of the target DNA inside the sample, with a limit-of-detection of 1 pM, from the hepatitis B virus. Reproduced with permission from ref. 46. Copyright 2013 IEEE.

bending of the cantilever [Fig. 6(a) and (b)]. Hence, the optical gadgets can be eliminated, allowing the integration of the cantilever with the readout circuitry. They demonstrated the detection of DNA from the hepatitis B virus after washing and drying of water molecules from the cantilever, with a sensitivity as low as 1 pM [Fig. 6(c)].

Another novel type of mechanical transducer in CMOSs is the surface acoustic wave (SAW) transducer [Fig. 2(e)], which detects the acoustic wave transmission pattern between two transducers. When the target binds with the immobilized probe in the acoustic wave transmission path (delay line), the properties of the output will change, thus allowing mass detection.[83] Tigli *et al.* proposed a SAW biosensor in CMOS technology to detect the cancer marker, human mammaglobin (hMAM).[55] By adopting a post-processing step, a piezoelectric zinc oxide layer can be deposited on the CMOS chip. This zinc oxide layer affects the resonant frequency of the SAW along the delay line, according to the mass attached to it, permitting the quantification of the hMAM biomarker.

NMR-based

Recently, nuclear magnetic resonance (NMR) has gained popularity for biomolecule detection. The underlying physics of NMR is the exchange of energy between the nuclear spins of the nuclei and the radio-frequency magnetic field in the presence of a static magnetic field. Similar to the magnetic sensing scheme, NMR-based biosensors rely on magnetic labels to selectively detect the target. Yet, they indirectly detect these magnetic labels from the ^{1}H NMR signals of aqueous samples. The spin–spin relaxation time of the NMR signals will be disturbed by the magnetization and the size of the magnetic nanoparticles.[84] The probe-decorated magnetic nanoparticles stay mono-dispersed before mixing with the target. After mixing with the target inside the samples, the probe binds with the target and thus the magnetic nanoparticles gather and form micro-clusters. These micro-clusters have a larger size and different magnetization, and thus the relaxation time of the sample will change accordingly. By detecting the NMR signals from the samples, the concentration of the target can be quantified from their spin–spin relaxation time. A NMR spiral sensing coil implemented by a top metal layer transduces between the electrical signals from the readout circuit and the magnetic field generated by the nuclear spins [Fig. 2(f)]. Compared to the direct magnetic sensing scheme, the NMR-based technique radically eases the hardware preparation, since immobilization is not required.

The versatility and flexibility of NMR-based biosensing enable different types of biomolecule assays. While NMR-based detection was originally performed with a discrete prototype,[85–91] significant efforts have evolved to integrate the electronics and detecting coil into a single CMOS chip for portable and low-cost assays. For instance, Sun *et al.* reported a one-chip NMR system to detect protein, cancer markers and bladder cancer cells inside 5 μL samples,[56] equipped

 This journal is © The Royal Society of Chemistry 2016

Open Access Article. Published on 09 September 2016. Downloaded on 1/4/2026 2:20:32 PM.
This article is licensed under a Creative Commons Attribution 3.0 Unported Licence.

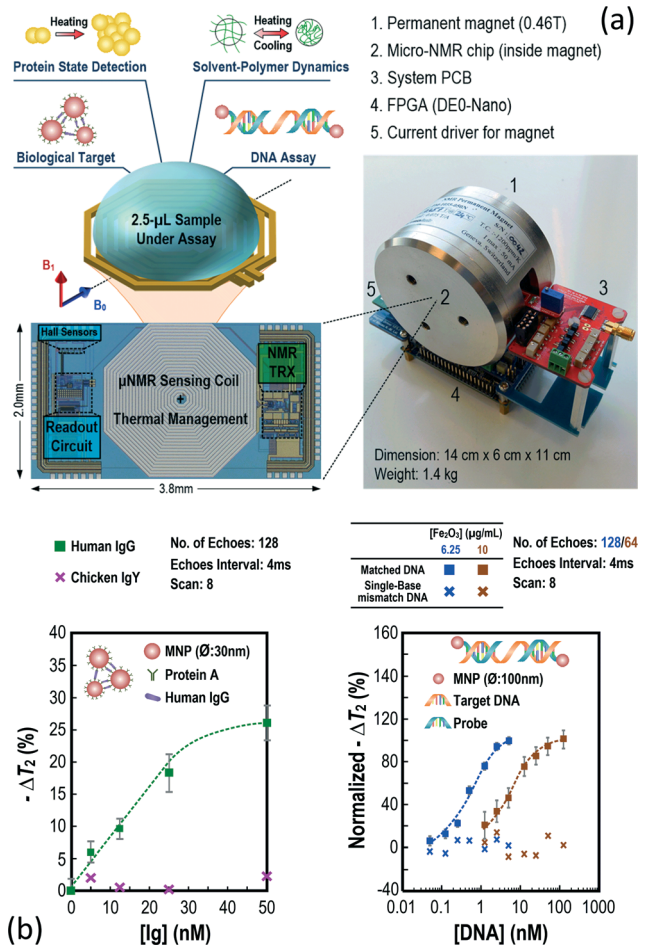

Fig. 7 The handheld micro-NMR relaxometer for chemical or biological assays. (a) The proposed micro-NMR platform. This consists of five main modules: 1. portable magnet for magnetizing the protons from the samples. 2. A micro-NMR chip for performing the NMR experiment. 3. System PCB for biasing and powering the chip. 4. The field programmable gate array for controlling the hardware and also communicating with the host (computer). 5 current driver to inject the current to the auxiliary coil of the magnet to stabilize the magnet field and safeguard the operation. The CMOS chip comprises an NMR transceiver, NMR sensing coil and Hall sensor to sense the magnetic field variation from the magnet. The sample under assay is put atop the sensing coil for analysis. Benefitting from the versatility of the NMR experiment, different assays such as biomolecule targeting and protein state analysis can be performed on this platform, rendering it suitable for healthcare, the food industry and colloidal applications. (b) The biomolecule targeting results. The platform can selectively detect the concentration of the target by analyzing the spin–spin relaxation time from the detected NMR signals. By entailing different probes, the platform is capable of detecting different kinds of biomolecules, such as human immunoglobulin G and DNA derived from *Enterococcus faecalis* without post-processing on the CMOS chip. Reproduced with permission from ref. 52. Copyright 2016 IEEE.

with a transceiver along with the sensing coil to perform the NMR experiment and enable lab-on-a-chip operation. Also, we demonstrated an integrated NMR system with an on-chip sensing coil and magnetic field stabilization module [Fig. 7(a)].[52] This stabilization module enhances the robustness of the platform against ambient variations, such as temperature. The functionality of the platform has been evinced by the detection of human immunoglobulin G and synthesized DNA from *Enterococcus faecalis* in 2.5 μL samples [Fig. 7(b) and (c)].

III. *In vitro* diagnostic applications

In vitro diagnosis focuses on analyzing targets from specimens. Different biological objects, such as protein, DNA or cell/bacteria, can be targeted. This section introduces assays with CMOS biosensors and their biological applications suitable for *in vitro* diagnosis, according to Table 1.

Immunoassay

The prevailing assay for detecting protein-based targets is the enzyme immunoassay. It is based on an enzyme-labeled antibody (antigen) to detect the target antibody (antigen). The most dominating method of enzyme immunoassay is the enzyme-linked immunosorbent assay (ELISA).[92] By observing a visual signal, such as a color change from an enzyme or fluorescent label, the concentration of a target inside a sample can be quantified. ELISA is referred as the golden standard in the clinical laboratory for a broad range of applications, such as dengue,[93] cancer markers,[94] and H5N1 influenza.[95]

Despite the popularity of ELISA in conventional laboratories, ELISA is labor-intensive and time-consuming, limiting its prevalence in resource-limited areas (*e.g.*, forest). In this regard, significant efforts have been focused on migrating the immunoassay to a CMOS chip for superior performance and small-form factor. Klapproth *et al.* demonstrated a multi-analyte CMOS sensor to measure multiple sandwich-ELISA reactions performed on the CMOS chip.[63] The chemiluminescence is recorded by the on-chip photodetector working in the reverse-bias region. This allows parallel detection of different biological targets, such as immunoglobulin E and myoglobin, and shows comparable results to the clinical protocols. Alternatively, Kuo *et al.* reported a smart CMOS assay system-on-chip platform for rapid blood screening with a Hall sensor to transduce the magnetic field generated by an on-chip magnetic coil to a voltage signal[62] [Fig. 8(a)]. An anodic aluminium oxide membrane filters the biomarkers from the blood sample. Then, the filtered sample is pumped to the Hall sensor array for immunoassay by the electrolytic electrodes [Fig. 8(b)]. With the bound magnetic particles, the magnetic field generated by the coil will be enhanced. The system is capable of detecting a biological target, such as tumor necrosis factor-α for anti-tumor response and N-terminal pro-brain natriuretic peptide for heart failure response, from whole blood [Fig. 8(c)].

DNA hybridization assay

Diagnosis with DNA biomolecules has a broad range of applications, such as mutation in DNA sequences for cancer

Open Access Article. Published on 09 September 2016. Downloaded on 1/4/2026 2:20:32 PM.
This article is licensed under a Creative Commons Attribution 3.0 Unported Licence.

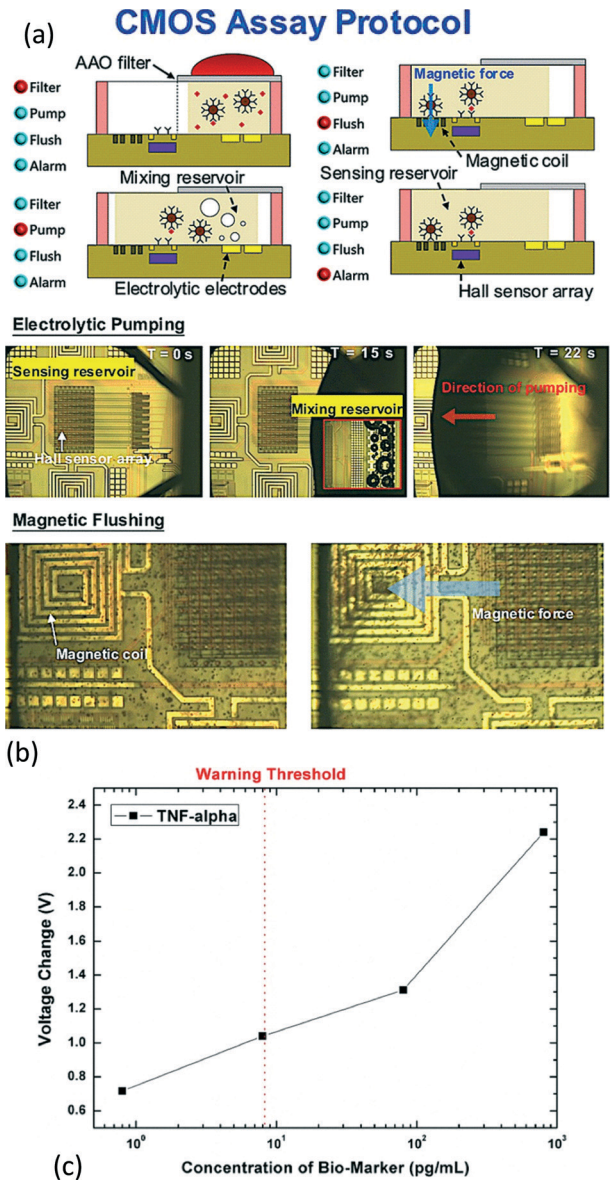

Fig. 8 Smart CMOS system-on-chip platform for rapid blood screening test for risk prediction. (a) The experimental procedure of the platform. Firstly, the blood under analysis is put atop the anodic aluminium oxide membrane. The biomarkers will be diffused to the mixing reservoir and separated from other blood cells (>1 μm). After filtration, the filtered sample in the mixing reservoir, together with the bio-functionalized magnetic bead, will be pumped to the sensing site by the force from the electrolytic pumping. Upon capturing by the coated antibody at the surface of the CMOS chips, the target and the magnetic bead will be seized, while the unbound magnetic bead will be flushed away by the magnetic force from the on-chip coil. Thus, the Hall sensor can sense the magnetic bead and identify the concentration of the targeted biomarker. (b) A photograph showing the electrolytic pumping and magnetic flushing. At first, the sample is on the right of the sensing reservoir. Then, a voltage is applied on the electrolytic electrodes and bubbles are formed as a consequence. The bubbles here induce a gas force and pump the sample to the sensing reservoir. After the sample arrives at the sensing site, the immobilized antibodies capture the targets and the magnetics beads. Then, the unbound magnetic beads will be flushed away by the on-chip coil. (c) The experimental result (TNF-alpha) of the immunoassay. The Hall sensor detects the target analyte from the magnetic beads on the sensing site. The system can detect 0.8 pg mL^{-1} to 80 ng mL^{-1} of TNF-alpha and NT-proBNP from whole blood. Reproduced with permission from ref. 62. Copyright 2015 IEEE.

prediction[96] and pathogen detection. Detection of the specific DNA is grounded on DNA hybridization detection. DNA hybridization is a molecular biology technique used to identify a sequence of interest, which is analogous to immunoassay. A single strand DNA complementary to the target DNA acts as a probe and is used to selectively detect the target. If the target DNA is complementary to the designated probe, DNA hybridization occurs and double-stranded DNA will be formed. Then, the detector will detect the designated signaling tag to quantify the target DNA inside the sample.

Conventionally, DNA detection relied on fluorescence-based detection similar to immunoassay.[97] This shares similar drawbacks with the immunoassay, such as bulky optical instruments. Thus, considerable efforts have been geared towards implementing the DNA assay tool with a CMOS chip for multifarious biological purposes. For instance, Jafari *et al.* proposed a nanostructured CMOS ultra-wideband label-free PCR-free DNA detection system.[50] This supports 54 channel

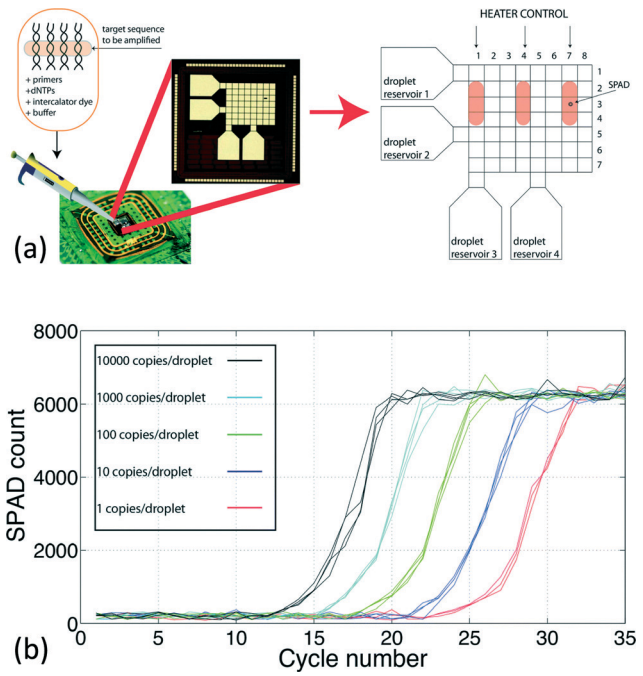

Fig. 9 Integrated qPCR system on CMOS chip. (a) The CMOS chip and illustrations of its functions. The chip has three main modules to enable on-chip qPCR. An electrowetting-on-dielectric device serves as an electronic-automated droplet management module to extract the target, PCR reagents, buffer, and intercalator dye from the reservoirs, and guides them to different electrodes for mixing and subsequent operations by applying a voltage on corresponding electrodes. A thermal module, which is formed by a resistive heater and temperature sensor, regulates the temperature of the droplets to perform thermal cycling for a polymerase-chain-reaction. A single photon avalanche diode is embodied on the CMOS chip to detect the fluorescent emission from the target DNA in real-time for qPCR. (b) Experimental results of the qPCR. The fluorescent signal from the sample increases with the PCR cycle. The qPCR system achieves a linear relationship between the cycle threshold and logarithm of the initial DNA concentration from 1 to 10 000 copies per 1.2 nL of droplets, resulting in a 40 000 fold reduction of the reagent consumption. Reproduced with permission from ref. 51. Copyright 2014 RSC Publishing.

 This journal is © The Royal Society of Chemistry 2016

Open Access Article. Published on 09 September 2016. Downloaded on 1/4/2026 2:20:32 PM.
This article is licensed under a Creative Commons Attribution 3.0 Unported Licence.

fast-scan cyclic voltammetry DNA analysis. The electrical-based transducing mechanism here enables the complete integration of the platform, including the transducers (electrodes), current readout circuit, waveform generator for cyclic voltammetry, and transmitter for communication. The system demonstrated label-free detection of prostate cancer synthetic DNA without DNA amplification, featuring a detection range from 10 aM to 10 μM. In another study, Norian *et al.* implemented an integrated CMOS quantitative-polymerase-chain-reaction (qPCR) lab-on-chip platform by integrating a thermal module, a digital microfluidic module and a single-photon avalanche diode (SPAD) on a single CMOS chip [Fig. 9(a)].[51] The proposed platform achieved fully integrated qPCR instrumentation, with proof-of-concept detection of DNA from *Staphylococcus aureus* with a detection limit down to 1 copy per 1.2 nL droplets, reducing the reagent consumption by 40 000× [Fig. 9(b)].

Cell/bacteria diagnosis

Cell level diagnosis also plays a significant role in the IVD field. An example is the counting of CD4+ T cells in human whole blood to spot the human immunodeficiency virus (HIV) infection. CD4+ T cells are a type of white blood cell that is essential to the human immune system. Upon infection by the HIV virus, the CD4+ T cells are depleted and thus the immune system is degenerated. An efficient approach to diagnosing and monitoring HIV infection is CD4+ T cell counting. Flow cytometry is the golden standard for counting CD4+ T cells.[98] The basic principle is to enumerate the CD4+ T cells passing through the detector during continuous flow of the sample. The appearance of the CD4+ T cells will alter the parameters of interest, such as impedance, or the light beam on the photodetector, such that the number of cells inside the samples can be counted. Yet, a conventional flow cytometer requires bulky detection tools and a large volume of sample. In this regard, Lee *et al.* proposed a CMOS impedance cytometer to monitor the flow inside the PDMS microchannel.[69] They utilized the cytometer to diagnose the rigidity of the red blood cells (RBC). A rigid RBC opposes deformation caused by shear stress in the medium, and is related to distinctive diseases, which offers a potential for micro-circulation study.

Another key application of cell-level diagnosis is cell monitoring for growth, cytotoxicity, and virus detection inside the cell. Monitoring the cellular activity (*i.e.*, cell division, apoptosis, and necrosis) using electronics enables real-time automated assay on designated cells, when compared with the traditional microscopic approach. There have been efforts to monitor the cells using different electronic-based techniques, such as impedance sensing and imaging for different diagnostic purposes. For instance, Chi *et al.* proposed a CMOS 3 × 3 multi-modal cell-assay platform for cellular assay [Fig. 10(a) and (b)].[76] Benefitting from the high integration level of the CMOS technology, different types of sensors, such as photodiodes, temperature sensors, and impedometers, are integrated within a single pixel, rendering it a promising platform for joint-modality cellular physiological monitoring. Various cells, such as ovarian cancer cells and human cardiomyocytes have been entailed for biological experiments and verification [Fig. 10(c)]. Recently, Laborde *et al.* reported a 256 × 256 nanocapacitor array for real-time imaging of microparticles and living cells on a CMOS chip.[75] By simultaneously exploring the benefits of CMOS technologies, they achieved label-free and high-throughput monitoring of different cancer cells with attofarad resolution on the sub-micrometer scale.

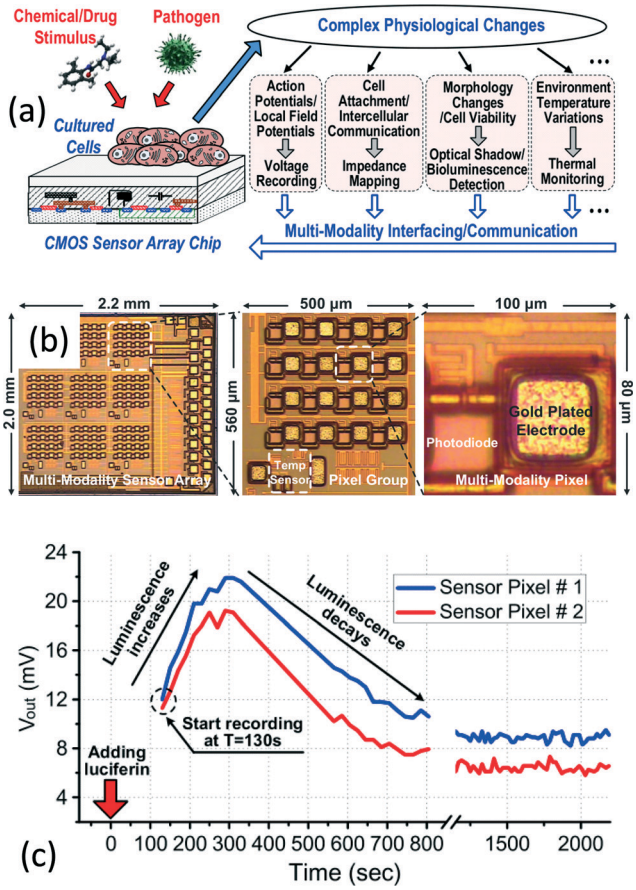

Fig. 10 CMOS multi-modal sensor array for cell-based assay. (a) Schematic of the multi-modal cell-based assay platform. The entire platform consists of a 3 × 3 sensor array and each pixel consists of a photodiode, a temperature sensor (shared within a pixel group), a voltage amplifier, and an impedance detector for multi-modal study and monitoring of the cultured cells exposed to drug or pathogen stimulation. (b) A micrograph of the CMOS cellular sensor chip. The chip contains 9 pixel groups for individual cell-based assay and each pixel group further contains 16 individual pixels. Each pixel is formed by a gold plated electrode for action potential and impedance reading with a photodiode. (c) Real-time experimental results from the bioluminescence experiment at 2 pixels. The human ovarian cancer cell emits luminescence upon the addition of luciferin, enabling verification of cell viability. The photodiode captures this bioluminescence and the readout circuit processes the signal for subsequent analysis. Reproduced with permission from ref. 76. Copyright 2015 IEEE.

Open Access Article. Published on 09 September 2016. Downloaded on 1/4/2026 2:20:32 PM.
This article is licensed under a Creative Commons Attribution 3.0 Unported Licence.

IV. Discussion and selection guide

Since there is high diversification of the characteristics and properties of CMOSs *in vitro* biosensors, as shown in Table 1, we aim to summarize a selection guide and provide a radar chart of each transducing method. Herein, we analyze and discuss the properties, requisites, and limitations of CMOS biosensors, based on their transducing mechanisms, evaluated in terms of the integration level, labeling scheme, hardware preparation, operation steps, and specificity.

Integration level

For cost and size minimization, the integration of all necessary hardware of the biosensor into a unified platform is desirable. Electrical-based detection is an ideal solution for sensing both small biomolecules (DNA and proteins) and large biological objects (cells and bacteria). External non-electronic gadgets (*e.g.*, light sources, optical filters, or magnets) can be avoided. Similarly, mechanical-based detection is a promising method of biosensing, except for the case of utilizing a laser beam for detecting cantilever deflection.[53] Traditionally, magnetic-based detection involves either a permanent magnet[49] or external coil[58] to magnetize and sense magnetic particles. Yet, there have been certain efforts to eliminate these external gadgets by implementing the coil-on-chip[62] or adopting the LC-oscillator[40] to sense magnetic particles. Optical-based biomolecule detection, especially for fluorescence, shares the same drawbacks as centralized benchtop assay, such as the need for excitation light sources. NMR-based detection, in this perspective, is difficult for integration since it involves a large permanent magnet (typical size of the magnet for NMR: 8 cm in diameter; 5.5 cm in height) for performing the NMR experiments. Furthermore, the magnetic field generated by the permanent magnet is temperature-dependent, and calibration is required to ensure proper operation.[52,89]

Labeling

The labeling process determines the effort and difficulties associated with preparing the sample and corresponding probes. Label-free assay is preferable, as it does not require complicated signal tags, such as fluorescence, redox-active molecules, and magnetic particle labeling on the sample and probe to detect the target. Electrical and mechanical-based detection are superior in this area since they both support label-free detection. While certain studies entailed redox tagging for signaling,[41] most of the electrical/mechanical-based biosensors are label-free, simplifying the sample preparation before the assay. On the other hand, NMR-based biosensors utilize magnetic particles functionalized with the capturing probe for detection. The labeling process restricts the experiments when compared with electrical/mechanical-based biosensors. Nevertheless, since surface functionalization only entails a probe, instead of a target, the sample under assay can remain unprocessed. Optical/magnetic-based biosensors involve attaching fluorescent, luminescent or magnetic labels on the target for assaying, which substantially increases the effort and cost of the assay. Yet, a sandwich-based bioassay technique can be applied to circumvent labeling the target to reduce the number of sample preparation steps.

Hardware preparation

Hardware preparation indicates the procedures required to prepare the hardware after receiving the standard CMOS chip from the foundry and before the assay, which include CMOS post-processing: etching, chemical deposition, or immobilization of the capturing probe. Certainly, an ideal biosensor should avoid these steps to reduce the cost and simplify the assay. NMR-based biosensors are promising in this regard as they do not entail any surface modification, plating or probe immobilization steps (*i.e.*, the chip is used as received). While the optical/magnetic-based biosensors do not necessarily involve post-processing on the CMOS chip, since there is no direct contact, immobilization of the probe on the substrate is still required. This substrate may be an external epoxy container, glass plate, or on-chip Au electrode. Electrical/mechanical-based biosensors involve complex post-processing steps to deposit a biocompatible Au layer on the pre-defined electrodes, and immobilize the necessary probe. Especially for the cantilever, the silicon substrate underneath has to be etched away to allow bending or oscillating of the cantilever. These post-processing steps greatly raise the cost and difficulty involved in preparing biosensors.

Operation

The operation denotes the procedures required to perform the assay, *e.g.*, washing and drying. An ideal CMOS biosensor should involve only a sample-loading step to detect the target. For small biomolecule sensing, the NMR-based biosensor stands out as a tantalizing solution since it does not encompass any washing step after the mixing of the probe and sample. Still, for cellular detection, a washing step is included to rinse off unbound magnetic particles. On the other hand, electrical-based detection has a facile operation procedure for small biomolecules. Despite certain studies involving a washing step after hybridization to remove the unbound target on the surface, the change in electrical properties upon hybridization can be detected without further washing steps. Fluorescent and magnetic-based biosensors encompass a washing step to remove the unbound molecule, similar to the conventional ELISA. Nevertheless, they are promising for cellular sensing, since the washing step is omitted in this case. Mechanical-based biosensing is confined by the operation procedures, since it entails both washing and drying steps to rinse off the unbound molecules, and drying of the surface of the cantilever. These steps are time-consuming and require considerable labor.

Specificity

The archetypal and ultimate goal of CMOS biosensors is to detect desired biomolecules in samples. Yet, for complex biological media (*e.g.*, blood plasma and serum), the sample

 This journal is © The Royal Society of Chemistry 2016

Open Access Article. Published on 09 September 2016. Downloaded on 1/4/2026 2:20:32 PM.
This article is licensed under a Creative Commons Attribution 3.0 Unported Licence.

matrix effect will incur non-specific binding and confound the detection limit of the system. For instance, albumin, the most abundant protein inside blood plasma, may exist with a concentration of 600 μM (*i.e.* ~1 billion times above the desired detection limit).[99] The non-specific binding of albumin with the probe leads to a background biological noise floor, creating a false positive on the output of the diagnostic tool. Additionally, other physical parameters, such as temperature or the pH of the sample, may affect the diagnosis. While these interferences can possibly be suppressed by hardware techniques, such as differential detection (*i.e.*, comparing the experimental result with a reference result), the additional measurement increases the hardware cost and the sample consumption. The specificity of optical-based and magnetic-based detection is outstanding as the detections rely on labeling process and multi-step protocols. Any undesired signaling tag will be removed from the sensing region after the rinsing step. In contrast, electrical-based detection is prone to the sample matrix effect, due to the non-specific absorption of other biomolecules.[100,101] Especially for EIS, the impedance is affected not only by non-specific absorption from the sample matrix, but also the constitution of the media (*i.e.*, conductivity of the media and permittivity of the cells). This poses a detrimental effect on the measurement. A mechanical-based detector is sensitive to non-specific binding of the biomolecule and ambient temperature interference. Yet, the washing and drying steps reduce the influence from non-specific binding. Finally, NMR-based detection, similar to magnetic-based detection, shows high specificity, ascribed to the adoption of surface functionalized magnetic nanoparticles. Yet, the spin–spin relaxation time of the sample correlates with the viscosity as well as the composition and state of the media (*i.e.* oxygenation of the blood sample[102]). This restricts direct measurement from complex media.

Summary

Electrical-based transducing mechanisms are generally the most widespread and favorable detection schemes for CMOS IVD tools, since they can provide label-free biomolecule detection and cellular monitoring without bulky external components, such as optical filters or permanent magnets. Furthermore, the ease of operation (*i.e.*, no washing and drying steps) promises fast assays and befits the PoC applications. Yet, the hardware preparation on CMOS chips and the necessity for direct contacts pose certain limits on electrical-based detection, especially when interfacing with other microfluidic networks.[103] Furthermore, the external influence requires delicate systematic design to achieve better specificity. Mechanical-based biomolecule detection, constrained by its complexity of hardware preparation and experimental procedure, shows limited exposure for CMOS IVD tools.

In contrast, despite the labeling step and non-integrated gadgets, optical-based detection is still popular for CMOS IVD tools, since the conventional laboratory protocols, such as ELISA and qPCR, can be transferred smoothly to the CMOS chip. This increases the consistency of the experimental results of CMOS IVD tools with the centralized benchtop assay. Its capability of detecting light transmittance also renders it a promising scheme for cellular assay. Alternatively, magnetic-based detection is similar to optical-based detection for biomolecule targeting, as both require labeling and several mixing and washing steps. The lack of magnetic substance inside the biological sample enables sensitive and specific biomolecule quantification for magnetic-based

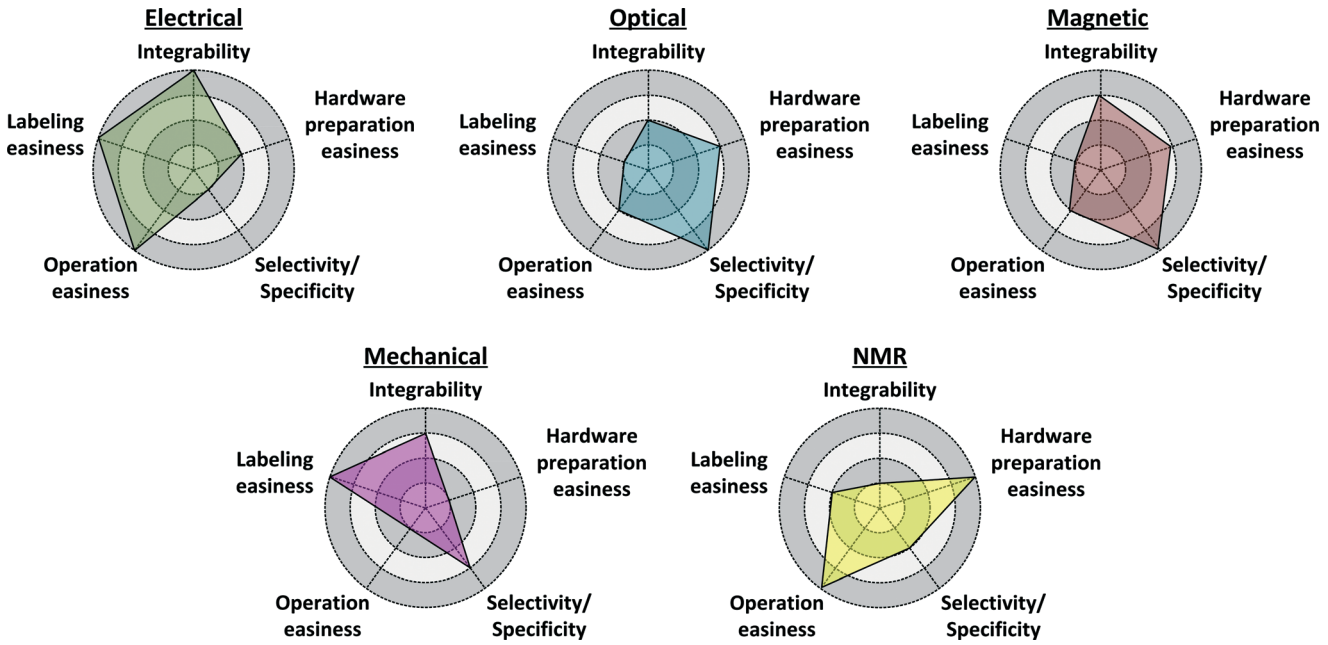

Fig. 11 A radar chart showing the conceptual requisites to perform *in vitro* diagnosis on biomolecule targets with different transducing mechanisms.

Open Access Article. Published on 09 September 2016. Downloaded on 1/4/2026 2:20:32 PM.
This article is licensed under a Creative Commons Attribution 3.0 Unported Licence.

detection. Furthermore, the high specificity of the labeling schemes for optical-based and magnetic-based detection guarantees the robustness of the systems against matrix effects from complex biological media. NMR-based detection is a promising solution for CMOS IVD tools when the preparations of the CMOS chip and sample beforehand have to be minimized. Also, the contactless properties of NMR facilitate the integration of the NMR electronics with sample management networks.[87,104] Yet, the relatively weak NMR signal limits the sensitivity of NMR-based detection and the permanent magnet hinders the miniaturization of the overall platform.

A conceptual radar chart is plotted in Fig. 11, showing, in general, the overall strengths and weaknesses of the above characteristics of the biosensors, using distinct transducing mechanisms. Obviously, there are many applications for *in vitro* diagnosis, especially for cellular level study (cell counting, monitoring, or flow cytometry), thus Fig. 11 is evaluated mainly on their performance for biomolecule (DNA and protein) targeting. Also, there are exceptional cases. For instance, Peng *et al.* reported an NMR-based label-free platform (with discrete electronics) for detecting malaria in whole blood by detecting the variation in spin–spin relaxation time of NMR signals from paramagnetic hemozoin particles.[105]

V. Conclusions and future prospects

Driven by the world's booming and longevous population in the coming century, there will be a huge market for efficient, low-cost and easy-to-use PoC devices for rapid yet sensitive *in vitro* diagnosis in both developed and developing countries. CMOS technology offers a platform to implement these IVD tools, which is attributed to its capability for monolithically integrating transducers and signal processing units on the same chip, which can be mass-produced to minimize the cost. Furthermore, benefitting from the continuous improvement of CMOS processes and post-processing techniques, a multifaceted variety of biosensors have been proposed with superior performances. There are different ways to achieve molecular and cellular biosensing on CMOS chips. The necessity and complexity of each transducing mechanism entails a balance of different design goals (*e.g.*, cost) and constraints. Thus, the development of an ideal CMOS biosensor should require profound knowledge, not only in microelectronics, but also in biology and chemistry, to secure successful multi-disciplinary research.

The advances in CMOS biosensors will continue with the downscaling of CMOS technology, offering a higher integration level, and better signal processing for a lower detection limit, and supporting more complex operations, such as next-generation sequencing.[106] Yet, the post-processing of the CMOS device should be limited and the labelling of the signaling tag should be avoided to suppress the manufacturing cost and the preparation time of the experiments, in order that the overall cost can be competitive with other PoC technologies, such as test-strip devices. Furthermore, it is also of importance to manage the sample matrix effects of biosensors from complex media and include different functions such as multiplexing[59] and DNA amplification[47,51] in an integrated platform, along with the CMOS biosensors. In addition, as sample management is still a challenge for CMOS chips, extra efforts should be entailed to seamlessly integrate the sample management network and the CMOS biosensor with the aid of channel microfluidic networks[107–109] or digital microfluidic arrays,[104,110] rendering these CMOS biosensors as truly lab-on-a-chip platforms. In our opinion, these CMOS biosensors will ultimately provide global patients with an efficient and powerful IVD solution to improve their living quality.

Acknowledgements

The authors thank Macao FDCT (SKL fund & 047/2014/A1) and the University of Macau for financial support.

References

1 D. C. H. Burgess, J. Wasseramn and C. A. Dahl, *Nature*, 2006, **444**(suppl. 1), 1–2.
2 P. Yager, G. J. Domingo and J. Gerdes, *Annu. Rev. Biomed. Eng.*, 2008, **10**, 107–144.
3 M. Zuiderwijk, H. J. Tanke, R. Sam Niedbala and P. L. A. M. Corstjens, *Clin. Biochem.*, 2003, **36**, 401–403.
4 X. Fu, Z. Cheng, J. Yu, P. Choo, L. Chen and J. Choo, *Biosens. Bioelectron.*, 2016, **78**, 530–537.
5 J. Li and J. Macdonald, *Lab Chip*, 2016, **16**, 242–245.
6 J. R. Choi, J. Hu, R. Tang, Y. Gong, S. Feng, H. Ren, T. Wen, X. Li, W. A. B. Wan Abas, B. Pingguan-Murphy and F. Xu, *Lab Chip*, 2016, **16**, 611–621.
7 M. La, S. M. Park and D. S. Kim, *Biomicrofluidics*, 2015, **9**, 014104.
8 B. S. Lee, Y. U. Lee, H.-S. Kim, T.-H. Kim, J. Park, J.-G. Lee, J. Kim, H. Kim, W. G. Lee and Y.-K. Cho, *Lab Chip*, 2011, **11**, 70–78.
9 J. Park, V. Sunkara, T.-H. Kim, H. Hwang and Y.-K. Cho, *Anal. Chem.*, 2012, **84**, 2133–2140.
10 W. S. Lee, V. Sunkara, J.-R. Han, Y.-S. Park and Y.-K. Cho, *Lab Chip*, 2015, **15**, 478–485.
11 G. A. Posthuma-Trumpie, J. Korf and A. van Amerongen, *Anal. Bioanal. Chem.*, 2009, **393**, 569–582.
12 *World development report: making services work for poor people*, World Bank, New York, NY, 2004.
13 *The top 10 causes of death*, http://www.who.int/mediacentre/factsheets/fs310/en/index2.html, (accessed 10th June, 2016).
14 *World population prospects: The 2015 revision*, United Nations, 2015.
15 A. Palangkaraya and J. Yong, *Int. J. Health Care Finance Econ.*, 2009, **9**, 391–402.
16 Z. Miller, *Investing in the future of medicine: A investor's guide to the in vitro diagnostics market*, http://www.forbes.com/sites/zackmiller/2014/02/12/investing-in-the-future-of-

 This journal is © The Royal Society of Chemistry 2016

Open Access Article. Published on 09 September 2016. Downloaded on 1/4/2026 2:20:32 PM.
This article is licensed under a Creative Commons Attribution 3.0 Unported Licence.

medicine-a-investors-guide-to-the-in-vitro-diagnostics-market/#9d6e5ea5feb4, (accessed 10th June, 2016).
17 S. K. Arya, C. C. Wong, Y. J. Jeon, T. Bansal and M. K. Park, *Chem. Rev.*, 2015, **115**, 5116–5158.
18 M. Crescentini, M. Bennati, M. Carminati and M. Tartagni, *IEEE Trans. Biomed. Circuits Syst.*, 2014, **8**, 278–292.
19 P. K. Drain, E. P. Hyle, F. Noubary, K. A. Freedberg, D. Wilson, W. R. Bishai, W. Rodriguez and I. V. Bassett, *Lancet Infect. Dis.*, 2014, **14**, 239–249.
20 J. P. Lafleur, A. Jönsson, S. Senkbeil and J. P. Kutter, *Biosens. Bioelectron.*, 2016, **76**, 213–233.
21 M. Drancourt, A. Michel-Lepage, S. Boyer and D. Raoult, *Clin. Microbiol. Rev.*, 2016, **29**, 429–447.
22 N. P. Pai, C. Vadnais, C. Denkinger, N. Engel and M. Pai, *PLoS Med.*, 2012, **9**, e1001306.
23 C. P. Y. Chan, W. C. Mak, K. Y. Cheung, K. K. Sin, C. M. Yu, T. H. Rainer and R. Renneberg, *Annu. Rev. Anal. Chem.*, 2013, **6**, 191–211.
24 A. Warsinke, *Anal. Bioanal. Chem.*, 2009, **393**, 1393–1405.
25 A. Niemz, T. M. Ferguson and D. S. Boyle, *Trends Biotechnol.*, 2011, **29**, 240–250.
26 V. Gubala, L. F. Harris, A. J. Ricco, M. X. Tan and D. E. Williams, *Anal. Chem.*, 2012, **84**, 487–515.
27 L. Gervais, N. de Rooij and E. Delamarche, *Adv. Mater.*, 2011, **23**, H151–H176.
28 J. Schmitz, *Nucl. Instrum. Methods Phys. Res., Sect. A*, 2007, **576**, 142–149.
29 C. G. Jakobson, U. Dinnar, M. Feinsod and Y. Nemirovsky, *IEEE Sens. J.*, 2002, **2**, 279–287.
30 A. H. D. Graham, S. M. Surguy, P. Langlois, C. R. Bowen, J. Taylor and J. Robbins, *Biosens. Bioelectron.*, 2012, **31**, 458–462.
31 J. M. Rothberg, W. Hinz, T. M. Rearick, J. Schultz, W. Mileski, M. Davey, J. H. Leamon, K. Johnson, M. J. Milgrew, M. Edwards, J. Hoon, J. F. Simons, D. Marran, J. W. Myers, J. F. Davidson, A. Branting, J. R. Nobile, B. P. Puc, D. Light, T. A. Clark, M. Huber, J. T. Branciforte, I. B. Stoner, S. E. Cawley, M. Lyons, Y. Fu, N. Homer, M. Sedova, X. Miao, B. Reed, J. Sabina, E. Feierstein, M. Schorn, M. Alanjary, E. Dimalanta, D. Dressman, R. Kasinskas, T. Sokolsky, J. A. Fidanza, E. Namsaraev, K. J. McKernan, A. Williams, G. T. Roth and J. Bustillo, *Nature*, 2011, **475**, 348–352.
32 A. Gao, N. Lu, Y. Wang and T. Li, *Sci. Rep.*, 2016, **6**, 22554.
33 J. Lee, J. Jang, B. Choi, J. Yoon, J.-Y. Kim, Y.-K. Choi, D. Myong Kim, D. Hwan Kim and S.-J. Choi, *Sci. Rep.*, 2015, **5**, 12286.
34 C. Stagni, C. Guiducci, L. Benini, B. Ricco, S. Carrara, B. Samori, C. Paulus, M. Schienle, M. Augustyniak and R. Thewes, *IEEE J. Solid-State Circuits*, 2006, **41**, 2956–2964.
35 M. Barbaro, A. Bonfiglio, L. Raffo, A. Alessandrini, P. Facci and I. Barák, *Sens. Actuators, B*, 2006, **118**, 41–46.
36 S. J. Han, H. Yu, B. Murmann, N. Pourmand and S. X. Wang, *IEEE Int. Solid-State Circuits Conf. (ISSCC) Dig. Tech. Papers*, 2007, 168–169.
37 E. Anderson, J. Daniels, H. Yu, T. Lee and N. Pourmand, *Proc. Instrum. Meas. Technol. Conf.*, 2008, 1631–1636.
38 B. Jang, P. Cao, A. Chevalier, A. Ellington and A. Hassibi, *IEEE Int. Solid-State Circuits Conf. (ISSCC) Dig. Tech. Papers*, 2009, 436–437.
39 T. C. D. Huang, S. Sorgenfrei, P. Gong, R. Levicky and K. L. Shepard, *IEEE J. Solid-State Circuits*, 2009, **44**, 1644–1654.
40 W. Hua, C. Yan, A. Hassibi, A. Scherer and A. Hajimiri, *IEEE Int. Solid-State Circuits Conf. (ISSCC) Dig. Tech. Papers*, 2009, 438–439.
41 P. M. Levine, P. Gong, R. Levicky and K. L. Shepard, *Biosens. Bioelectron.*, 2009, **24**, 1995–2001.
42 A. Manickam, A. Chevalier, M. McDermott, A. D. Ellington and A. Hassibi, *IEEE Trans. Biomed. Circuits Syst.*, 2010, **4**, 379–390.
43 H. Jafari, L. Soleymani and R. Genov, *IEEE Trans. Biomed. Circuits Syst.*, 2012, **6**, 468–478.
44 K. H. Lee, S. Choi, J. O. Lee, J. B. Yoon and G. H. Cho, *IEEE Int. Solid-State Circuits Conf. (ISSCC) Dig. Tech. Papers*, 2012, 120–122.
45 M. Barbaro, A. Caboni, D. Loi, S. Lai, A. Homsy, P. D. van der Wal and N. F. de Rooij, *Sens. Actuators, B*, 2012, **171–172**, 148–154.
46 Y. J. Huang, C. W. Huang, T. H. Lin, C. T. Lin, L. G. Chen, P. Y. Hsiao, B. R. Wu, H. T. Hsueh, B. J. Kuo, H. H. Tsai, H. H. Liao, Y. Z. Juang, C. K. Wang and S. S. Lu, *IEEE Trans. Biomed. Circuits Syst.*, 2013, **7**, 820–831.
47 C. Toumazou, L. M. Shepherd, S. C. Reed, G. I. Chen, A. Patel, D. M. Garner, C.-J. A. Wang, C.-P. Ou, K. Amin-Desai, P. Athanasiou, H. Bai, I. M. Q. Brizido, B. Caldwell, D. Coomber-Alford, P. Georgiou, K. S. Jordan, J. C. Joyce, M. La Mura, D. Morley, S. Sathyavruthan, S. Temelso, R. E. Thomas and L. Zhang, *Nat. Methods*, 2013, **10**, 641–646.
48 C.-W. Huang, Y.-J. Huang, P.-W. Yen, H.-H. Tsai, H.-H. Liao, Y.-Z. Juang, S.-S. Lu and C.-T. Lin, *Lab Chip*, 2013, **13**, 4451–4459.
49 A. Pai, A. Khachaturian, S. Chapman, A. Hu, H. Wang and A. Hajimiri, *Analyst*, 2014, **139**, 1403–1411.
50 H. M. Jafari, K. Abdelhalim, L. Soleymani, E. H. Sargent, S. O. Kelley and R. Genov, *IEEE J. Solid-State Circuits*, 2014, **49**, 1223–1241.
51 H. Norian, R. M. Field, I. Kymissis and K. L. Shepard, *Lab Chip*, 2014, **14**, 4076–4084.
52 K. M. Lei, H. Heidari, P. I. Mak, M. K. Law, F. Maloberti and R. P. Martins, *IEEE Int. Solid-State Circuits Conf. (ISSCC) Dig. Tech. Papers*, 2016, 474–475.
53 C. H. Chen, R. Z. Hwang, L. S. Huang, S. M. Lin, H. C. Chen, Y. C. Yang, Y. T. Lin, S. A. Yu, Y. S. Lin, Y. H. Wang, N. K. Chou and S. S. Lu, *IEEE Trans. Biomed. Eng.*, 2009, **56**, 462–470.
54 N. Sun, Y. Liu, H. Lee, R. Weissleder and D. Ham, *IEEE J. Solid-State Circuits*, 2009, **44**, 1629–1643.
55 O. Tigli, L. Bivona, P. Berg and M. E. Zaghloul, *IEEE Trans. Biomed. Circuits Syst.*, 2010, **4**, 62–73.
56 N. Sun, T. J. Yoon, H. Lee, W. Andress, R. Weissleder and D. Ham, *IEEE J. Solid-State Circuits*, 2011, **46**, 342–352.
57 S. Gambini, K. Skucha, P. P. Liu, J. Kim and R. Krigel, *IEEE J. Solid-State Circuits*, 2013, **48**, 302–317.

Open Access Article. Published on 09 September 2016. Downloaded on 1/4/2026 2:20:32 PM.
This article is licensed under a Creative Commons Attribution 3.0 Unported Licence.

58 D. A. Hall, R. S. Gaster, K. A. A. Makinwa, S. X. Wang and B. Murmann, *IEEE J. Solid-State Circuits*, 2013, **48**, 1290–1301.
59 L. Sandeau, C. Vuillaume, S. Contie, E. Grinenval, F. Belloni, H. Rigneault, R. M. Owens and M. B. Fournet, *Lab Chip*, 2015, **15**, 877–881.
60 C. Sapsanis, S. Sivashankar, H. Omran, U. Buttner and K. N. Salama, *Proc IEEE Int. Midwest Symp. Circuits Syst.*, 2015, 1–4.
61 L. Y. Hong, S. McManus, H. Yang and K. Sengupta, *Proc. Symp. VLSI circuits*, 2015, C206–C207.
62 P. H. Kuo, J. C. Kuo, H. T. Hsueh, J. Y. Hsieh, Y. C. Huang, T. Wang, Y. H. Lin, C. T. Lin, Y. J. Yang and S. S. Lu, *IEEE Trans. Biomed. Circuits Syst.*, 2015, **9**, 790–800.
63 H. Klapproth, S. Bednar, J. Baader, M. Lehmann, I. Freund, T. Brandstetter and J. Rühe, *Sens. Biosensing Res.*, 2015, **5**, 117–122.
64 Y. Zheng, N. Shang, P. S. Haddad and M. Sawan, *IEEE Trans. Biomed. Circuits Syst.*, 2016, **10**, 477–486.
65 S. B. Prakash and P. Abshire, *IEEE Sens. J.*, 2007, **7**, 440–447.
66 S. B. Prakash and P. Abshire, *Biosens. Bioelectron.*, 2008, **23**, 1449–1457.
67 E. P. Dupont, E. Labonne, Y. Maruyama, C. Vandevyver, U. Lehmann, M. A. M. Gijs and E. Charbon, *Sens. Actuators, B*, 2012, **174**, 609–615.
68 Y. Chen, C. C. Wong, T. S. Pui, R. Nadipalli, R. Weerasekera, J. Chandran, H. Yu and A. R. A. Rahman, *Sens. Actuators, B*, 2012, **173**, 903–907.
69 K. H. Lee, J. Nam, S. Choi, H. Lim, S. Shin and G. H. Cho, *IEEE Int. Solid-State Circuits Conf. (ISSCC) Dig. Tech. Papers*, 2012, 304–306.
70 H. Wang, A. Mahdavi, D. A. Tirrell and A. Hajimiri, *Lab Chip*, 2012, **12**, 4465–4471.
71 T. Saeki, M. Hosokawa, T. Lim, M. Harada, T. Matsunaga and T. Tanaka, *PLoS One*, 2014, **9**, e89011.
72 P. Murali, I. Izyumin, D. Cohen, J. C. Chien, A. M. Niknejad and B. Boser, *IEEE Int. Solid-State Circuits Conf. (ISSCC) Dig. Tech. Papers*, 2014, 422–423.
73 M. Roy, G. Jin, D. Seo, M.-H. Nam and S. Seo, *Sens. Actuators, B*, 2014, **201**, 321–328.
74 K. Niitsu, S. Ota, K. Gamo, H. Kondo, M. Hori and K. Nakazato, *IEEE Trans. Biomed. Circuits Syst.*, 2015, **9**, 607–619.
75 C. Laborde, C. Pittino, H. A. Verhoeven, S. G. Lemay, L. Selmi, M. A. Jongsma and F. P. Widdershoven, *Nat. Nanotechnol.*, 2015, **10**, 791–795.
76 T. Chi, J. S. Park, J. C. Butts, T. A. Hookway, A. Su, C. Zhu, M. P. Styczynski, T. C. McDevitt and H. Wang, *IEEE Trans. Biomed. Circuits Syst.*, 2015, **9**, 801–814.
77 K. T. Chang, Y. J. Chang, C. L. Chen and Y. N. Wang, *Electrophoresis*, 2015, **36**, 413–419.
78 J. C. Love, L. A. Estroff, J. K. Kriebel, R. G. Nuzzo and G. M. Whitesides, *Chem. Rev.*, 2005, **105**, 1103–1169.
79 A. Manickam, C. A. Johnson, S. Kavusi and A. Hassibi, *Sensors*, 2012, **12**, 14467.
80 C. Berggren, P. Stalhandske, J. Brundell and G. Johansson, *Electroanalysis*, 1999, **11**, 156–160.
81 J. Enderlein, T. Ruckstuhl and S. Seeger, *Appl. Opt.*, 1999, **38**, 724–732.
82 M. Alvarez and L. M. Lechuga, *Analyst*, 2010, **135**, 827–836.
83 H. Wohltjen and R. Dessy, *Anal. Chem.*, 1979, **51**, 1458–1464.
84 C. Min, H. L. Shao, M. Liong, T. J. Yoon, R. Weissleder and H. Lee, *ACS Nano*, 2012, **6**, 6821–6828.
85 L. Josephson, J. M. Perez and R. Weissleder, *Angew. Chem.*, 2001, **113**, 3304–3306.
86 J. M. Perez, L. Josephson, T. O'Loughlin, D. Hogemann and R. Weissleder, *Nat. Biotechnol.*, 2002, **20**, 816–820.
87 H. Lee, E. Sun, D. Ham and R. Weissleder, *Nat. Med.*, 2008, **14**, 869–874.
88 I. Koh, R. Hong, R. Weissleder and L. Josephson, *Angew. Chem., Int. Ed.*, 2008, **47**, 4119–4121.
89 D. Issadore, C. Min, M. Liong, J. Chung, R. Weissleder and H. Lee, *Lab Chip*, 2011, **11**, 2282–2287.
90 M. Liong, A. N. Hoang, J. Chung, N. Gural, C. B. Ford, C. Min, R. R. Shah, R. Ahmad, M. Fernandez-Suarez, S. M. Fortune, M. Toner, H. Lee and R. Weissleder, *Nat. Commun.*, 2013, **4**, 1–9.
91 C. M. Castro, A. A. Ghazani, J. Chung, H. L. Shao, D. Issadore, T. J. Yoon, R. Weissleder and H. Lee, *Lab Chip*, 2014, **14**, 14–23.
92 E. Engvall and P. Perlmann, *Immunochemistry*, 1971, **8**, 871–874.
93 R. W. Peeling, H. Artsob, J. L. Pelegrino, P. Buchy, M. J. Cardosa, S. Devi, D. A. Enria, J. Farrar, D. J. Gubler, M. G. Guzman, S. B. Halstead, E. Hunsperger, S. Kliks, H. S. Margolis, C. M. Nathanson, V. C. Nguyen, N. Rizzo, S. Vazquez and S. Yoksan, *Nat. Rev. Microbiol.*, 2010, S30–S37.
94 N. Scholler, M. Crawford, A. Sato, C. W. Drescher, K. C. O'Briant, N. Kiviat, G. L. Anderson and N. Urban, *Clin. Cancer. Res.*, 2006, **12**, 2117–2124.
95 S. Velumani, H.-T. Ho, F. He, S. Musthaq, M. Prabakaran and J. Kwang, *PLoS One*, 2011, **6**, e20737.
96 C. Kandoth, M. D. McLellan, F. Vandin, K. Ye, B. Niu, C. Lu, M. Xie, Q. Zhang, J. F. McMichael, M. A. Wyczalkowski, M. D. M. Leiserson, C. A. Miller, J. S. Welch, M. J. Walter, M. C. Wendl, T. J. Ley, R. K. Wilson, B. J. Raphael and L. Ding, *Nature*, 2013, **502**, 333–339.
97 M. Schena, D. Shalon, R. W. Davis and P. O. Brown, *Science*, 1995, **270**, 467–470.
98 H. Shafiee, S. Wang, F. Inci, M. Toy, T. J. Henrich, D. R. Kuritzkes and U. Demirci, *Annu. Rev. Med.*, 2015, **66**, 387–405.
99 J. L. Arlett, E. B. Myers and M. L. Roukes, *Nat. Nanotechnol.*, 2011, **6**, 203–215.
100 T. Bryan, X. Luo, P. R. Bueno and J. J. Davis, *Biosens. Bioelectron.*, 2013, **39**, 94–98.
101 J. T. Kirk, N. D. Brault, T. Baehr-Jones, M. Hochberg, S. Jiang and D. M. Ratner, *Biosens. Bioelectron.*, 2013, **42**, 100–105.
102 K. R. Thulborn, J. C. Waterton, P. M. Matthews and G. K. Radda, *Biochim. Biophys. Acta*, 1982, **714**, 265–270.
103 E. Ghafar-Zadeh and M. Sawan, *IEEE Trans. Biomed. Circuits Syst.*, 2007, **1**, 270–277.
104 K.-M. Lei, P.-I. Mak, M.-K. Law and R. P. Martins, *Analyst*, 2015, **140**, 5129–5137.

 This journal is © The Royal Society of Chemistry 2016

105 W. K. Peng, T. F. Kong, C. S. Ng, L. Chen, Y. Huang, A. A. S. Bhagat, N.-T. Nguyen, P. R. Preiser and J. Han, *Nat. Med.*, 2014, **20**, 1069–1073.
106 D. A. Hall, J. S. Daniels, B. Geuskens, N. Tayebi, G. M. Credo, D. J. Liu, H. Li, K. Wu, X. Su, M. Varma and O. H. Elibol, *IEEE Int. Solid-State Circuits Conf. (ISSCC) Dig. Tech. Papers*, 2016, 288–289.
107 Y. Huang and A. J. Mason, *Lab Chip*, 2013, **13**, 3929–3934.
108 R. R. Singh, L. Leng, A. Guenther and R. Genov, *IEEE J. Solid-State Circuits*, 2012, **47**, 2822–2833.
109 X. Liu, L. Li and A. J. Mason, *Philos. Trans. R. Soc., A*, 2014, 372.
110 G. Wang, D. Teng, Y. T. Lai, Y. W. Lu, Y. Ho and C. Y. Lee, *IET Nanobiotechnol.*, 2014, **8**, 163–171.

Open Access Article. Published on 09 September 2016. Downloaded on 1/4/2026 2:20:32 PM.
This article is licensed under a Creative Commons Attribution 3.0 Unported Licence.